



# STRATUS CONSULTING

## **Climate Change in Park City: An Assessment of Climate and Snowpack Impacts**

*Prepared for:*

Brent Giles  
Park City Mountain Resort  
PO Box 39  
Park City, UT 84060

**Climate Change in Park City:  
An Assessment of Climate  
and Snowpack Impacts**

*Prepared for:*

Brent Giles  
Park City Mountain Resort  
PO Box 39  
Park City, UT 84060

*Prepared by:*

Brian Lazar  
Stratus Consulting Inc.  
PO Box 4059  
Boulder, CO 80306-4059  
(303) 381-8000

*and*

Mark Williams  
Institute of Arctic and Alpine Research (INSTAAR)  
University of Colorado at Boulder

January 5, 2007  
SC11026

---

## Executive Summary

As atmospheric greenhouse gas (GHG) concentrations rise over this century and the climate continues to change, Park City is likely to warm substantially. Here, we present the results of a study for the Park City Mountain Resort using a site-specific technique for estimating potential changes in snow properties in response to future climate change scenarios. This report also addresses operational issues such as the ability to open on Thanksgiving, top-of-mountain snow depths during the Christmas holidays, and whether future ski seasons may end before the highly profitable spring break period in late March.

Specific objectives for this study were to estimate the length of the ski season, the timing of snowpack buildup and melt, and daily values of snow depth and coverage, from the bottom to the top of the mountain, for the years 2030, 2075, and 2100. This report presents the methods and results of climate model projections for a range of GHG emission scenarios, and the effects of projected climate change on snowpack characteristics for the Park City ski area.

### Climate

The term “climate change” refers broadly to the changes in climate that are being exacerbated by the increasing atmospheric concentrations of GHGs. We create scenarios as tools to help us understand how regional climates may change and to understand how sensitive systems may be affected by climate change. Scenarios are plausible combinations of conditions that can represent possible future situations.

For this study, we developed scenarios for three periods: the 2030s, the 2070s, and the 2100s. These time periods are not selected to predict weather in a particular future year, but to estimate how average climate conditions may change. The 2030s are within the “foreseeable future” and planning horizons for some stakeholders, the 2070s capture mid-term climate change, and the 2100s capture long-term climate change. We project out to 2100 because it is likely that the current path of GHG emissions will lead to substantial changes in climate at least that far out into the future (although reduction of emissions could substantially reduce climate change over this century).

Future changes in GHG emissions depend on many factors, including population growth, economic growth, technology, government, and society. Out of seven scenarios developed by the Intergovernmental Panel on Climate Change (IPCC), we selected four to use for the Park City study. Since likelihoods are not given for these scenarios, we use a range of them to reflect a wide range of potential future GHG concentrations.

We used three modeling approaches to examine potential future climate. The first is the “MAGICC/SCENGEN tool,” which evaluates climate change estimates over General Circulation Model (GCM) grid boxes that are 5° across, roughly 300 miles in length and width. We used the following five GCMs that best simulate current climate over western North America:

- ▶ CSIRO – Australia
- ▶ ECHAM3 – Max Planck Institute for Meteorology, Germany
- ▶ ECHAM4 – Max Planck Institute for Meteorology, Germany
- ▶ HadCM2 – Hadley Model, United Kingdom Meteorological Office
- ▶ HadCM3 – Hadley Model, United Kingdom Meteorological Office.

We examined climate projections from MAGICC/SCENGEN using each of the five GCMs independently, and using an average of output from the five GCMs.

To obtain increased spatial resolution of changes in climate in the Park City area, we used two additional modeling approaches. One is the output from a regional climate model (RCM). RCMs are high-resolution climate models that are built for a region, e.g., the United States, and are “nested” within a GCM. We used the RCM “MM5,” which has grid boxes 36 kilometers (about 20 miles) across. The model is “nested” in the Parallel Climate Model (PCM). We refer to this model run as the PCM RCM.

The second high-resolution modeling approach is called statistical downscaling. We developed the Statistical Downscaling Model (SDSM), which uses the statistical relationship between variables in a GCM and observed climate at a specific location such as a weather station. The approach assumes that the statistical relationship between the large-scale climate variables in a GCM and a specific location will not change with climate change. The advantage is that statistical downscaling can be used to develop a scenario for a specific location. For this study, we developed a scenario for the weather station located near the mid-mountain of the Park City ski area.

## Climate Results

All of the emission scenarios project a substantial increase in temperatures for the region over the next 100 years. The degree of warming is most sensitive to assumptions about GHG emissions and the modeling approach used. Different assumptions about emissions result in projected warming ranging from 3.3° to 8.4°C (5.9° to 15.1°F) in Park City by 2100. This implies that by 2100, Park City’s climate will resemble the current climate of Salt Lake City. Warming is projected to be more pronounced during the summer months than during the winter months. On average, the models project a decrease in annual precipitation. This is true regardless of the emissions scenario or modeling approach. However, due to variability between models, it is uncertain whether precipitation will decrease over the 21st century.

## Mountain Snow

We used the Snowmelt Runoff Model (SRM), developed and maintained by the U.S. Department of Agriculture Agricultural Research Service, to examine snowpack characteristics in the Park City ski area. SRM requires geographic information systems (GIS) information (including a digital elevation model, land use/land cover, and estimates of snow cover) for implementation. The model area is sub-divided into elevation zones, which enables the SRM to generate refined estimates of snowpack coverage and melt in areas with large vertical relief, such as the Park City ski area.

We used the SRM to estimate the length of the ski season, the timing of snowpack accumulation and melt, and the snow depth and coverage (derived from satellite imagery) at a given time. The spatial extent modeled for this study was dictated by the current (2006) Park City ski area property boundaries. Our modeled area spanned a vertical distance of approximately 1,067 m (3,500 ft), ranging from the base area elevation of 2,100 m (6,890 ft) to the highest elevation within the ski area property at 3,170 m (10,400 ft). We modeled the area in four elevation zones averaging 265 m (872 ft) in height.

An examination of the historical data, combined with an analysis of the availability of high-resolution images available during the winter months, led us to choose the season of 2000-2001 as our baseline of historical average conditions. We first ran SRM to simulate snow and snowmelt patterns for the 2001 water year, and then modeled future climate change scenarios by scaling observed temperature and precipitation records by the projected monthly changes, unique to each climate scenario.

## Mountain Snow Results

Using the climate change scenarios and the SRM, we estimate that the date when snow starts to accumulate at the base area will be delayed at least four weeks, and some scenarios predict no accumulation at all by 2100. This change in snow accumulation will be caused by an increase in air temperature. Thanksgiving and spring break snow depths at the base area are projected to be at or near zero for all scenarios in 2075. For the high-emission scenario in 2075, there is unlikely to be a persistent seasonal snowpack at the base area, and the snowline is projected to move up to approximately 2,900 m (9,500 ft). The top of the ski area will maintain skiable snow throughout the ski season in all but the highest emissions scenario, although snow depths are reduced by 15 to 65% compared to historical observations. By 2100, only the low-emission and SDSM scenarios project skiable snow at the base area, and only during December through February. Results for the mid-emission scenario for 2100 indicate that a persistent snowpack will only exist for the upper quarter of the mountain. For the high-emission scenario by 2100, there will be no persistent snow coverage at all.

An examination of the snowpack projections reveals that snowpack begins to be substantially impacted when winter temperatures warm more than approximately 2° to 3°C (4° to 5°F), regardless of scenario or year that threshold is reached. GCM results show that warming in the North American Rocky Mountains is approximately one-third greater than the global mean temperature (GMT). This implies Park City could experience a 2°C warming compared to a GMT warming of only 1.3°C (2.4°F). Such an increase in temperature could be reached by mid-century.

It is unlikely that early season reductions in snowpack can be offset with snowmaking by 2075, since according to the models, temperatures do not become cold enough for snowmaking until late November to early December. Additional snowmaking later into the winter months, however, could bolster the snowpack enough to maintain skiable snow later into the spring break season. The economic implications of additional snowmaking, and other potential adaptation strategies, such as downloading skiers in the spring, should be evaluated by ski area owners and operators in the face of a changing climate.

## 1. Introduction

There has long been concern regarding the potential impacts of climate change on a variety of snow dependent uses, from water resource supply to ski area operation.<sup>1</sup> An increasing number of hydrologic modeling studies have investigated the potential effects of climate change on snowmelt runoff volume and timing.<sup>2</sup> Other studies have analyzed the effects of potential climate change on ski areas and winter tourism; all project negative consequences for the industry.<sup>3</sup>

Operational managers of ski resorts need to be able to address issues such as the ability to open on Thanksgiving, top-of-mountain snow depths during the Christmas holidays, and the likelihood of ski seasons ending before the highly profitable spring break period in late March. Similarly, towns and businesses that depend on ski areas for their economic viability need specific information on how skiing and winter tourism may change in the future so they can make economic adjustments.

---

1. Tegart et al., 1990; Watson et al., 1996; National Assessment Synthesis Team, 2000; McCarthy et al., 2001.

2. Leavesley et al., 1992; McCabe and Hay, 1995; Rango and Martinec, 1997, 1999, 2000; Seidel et al., 1998; Barnett et al., 2005; Mote et al., 2005.

3. Galloway, 1988; McBoyle and Wall, 1992; König, 1998; Hennessy et al., 2003; Scott et al., 2003, Forthcoming; Scott and Jones, 2005; AGCI, 2006; Climate Impacts Group, 2006; Nolin and Daly, Forthcoming.

To estimate how the length and quality of the snow season in Park City, Wasatch Mountains of north central Utah, may change in the short-term and long-term future, Stratus Consulting used future GHG emissions scenarios, several existing climate change models, and the SRM<sup>4</sup> to predict potential future scenarios. The SRM combines a physically based approach to understanding snow dynamics with climate drivers that are compatible with the output of climate models, particularly air temperature and precipitation. In this report, we present projections of future emissions scenarios and their effects on climate and snow characteristics, including the length of the ski season, the timing of snowpack buildup and melt, and daily values of snow depth and coverage from the bottom to the top of the mountain. We present results for the years 2030, 2075, and 2100, to represent a near-term and two long-term forecasts. The 2030s are within the “foreseeable future” and planning horizons for some stakeholders, the 2070s capture mid-term climate change, and the 2100s capture long-term climate change.

Based on the model results, we found that projected increased GHG concentrations in the atmosphere will change Park City’s climate substantially. Temperatures are likely to rise and precipitation amount, timing, intensity, and variability will change. How precipitation and variability will change remains uncertain.

## 2. Overview of Climate Change

### 2.1 Background

The term “climate change” refers broadly to changes in climate that are being exacerbated by the increasing atmospheric concentrations in GHGs.<sup>5</sup> These GHGs include emissions of carbon dioxide (CO<sub>2</sub>) from fossil fuel combustion and land use change, methane (CH<sub>4</sub>) from waste disposal and energy resource development, nitrous oxide (N<sub>2</sub>O) from agriculture and industrial operations, and halocarbons used mainly by industry and for refrigeration.

---

4. Martinec, 1975; Martinec et al., 1994; model and documentation available: <http://hydrolab.arsusda.gov/cgi-bin/srmhome>.

5. For a more detailed discussion of climate change science, such as descriptions of the greenhouse effect, readers are encouraged to go to the report by the IPCC (Houghton et al., 2001). The IPCC was created by the United Nations and World Meteorological Organization to provide advice on the state of the science to policy makers. Every five to seven years, the IPCC issues a comprehensive summary on the latest consensus views about climate change science, environmental and socioeconomic impacts and the potential for adaptation, and options for lessening future change through various strategies for emissions reduction (i.e., mitigation). All of their assessment reports on how climate will change can be found at <http://www.ipcc.ch/pub/spm22-01.pdf>.

The IPCC has found that climate is changing. Averaged around the world, annual mean temperatures rose by 0.6°C +/- 0.2°C (1.1°F +/- 0.36°F) over the last 100 years, and other aspects of climate such as precipitation patterns have also changed. Careful analysis led the panel to conclude that human activities, including fossil fuel burning and deforestation, are responsible for at least half of the increase in the annual average temperature around the world in the last half century.

The IPCC Third Assessment Report (TAR; Houghton et al., 2001) projected that, averaged around the world, the annual mean temperature from 1990 to 2100 is likely to rise by between 1.4° and 5.8°C (2.5° to 10.4°F). The change in regional temperatures will vary considerably from place to place. The TAR (Houghton et al., 2001, p. 13) concluded the following:

Based on recent global model simulations, it is very likely<sup>6</sup> that nearly all land areas will warm more rapidly than the global average, particularly those at northern high latitudes in the cold season. Most notable of these is the warming in the northern regions of North America, and northern and central Asia, which exceeds global mean warming in each model by more than 40%.

Knowing that temperatures are projected to increase allows a number of conclusions to be drawn about changes in related phenomena:

- ▶ *Snow will melt earlier in the year.* For regions dependent on runoff from snowpack into rivers and lakes, peak runoff is likely to be earlier in the year, with much less snowmelt contributing to streamflow during late spring and summer. Higher temperatures are also likely to cause more precipitation to come as rain rather than snow during the year.
- ▶ *Evaporation will increase.* Higher temperatures generally accelerate evaporation. This is likely to lead to more intense droughts and more intense heavy precipitation events. The IPCC also concluded that the duration and intensity of midsummer droughts are likely to increase in interior, midcontinental areas (such as Central Asia), but results are inconclusive for other regions.

Global average precipitation will increase, but precipitation will not increase everywhere or in all seasons. The IPCC (Houghton et al., 2001, p. 13) states the following about regional precipitation patterns:

By the second half of the 21st century, it is likely that precipitation will have increased over northern mid- to high latitudes and Antarctica in winter. At low latitudes there are both regional increases and decreases over land areas.

---

6. IPCC defines “virtually certain” as having at least a 99% chance of happening, “very likely” as having a 90 to 99% chance of happening, and “likely” as having a 66 to 90% chance of happening.

Climate models tend to show increases in precipitation over very high latitudes and in equatorial regions. These changes are consistent with theoretical understanding about the results of an intensification of the global hydrological cycle. The climate models also tend to project decreases in precipitation in the Mediterranean, Mexico, and the southwestern United States.

## 2.2 Recent Climate Trends

In addition to evaluating the range of future climate scenarios, we investigated trends in observed historical data. The climate in the Park City region has been changing in recent decades, and here we review the historical temperature records of weather stations with reliable long-term records. In each of the following plots, the regression lines indicate the point slope estimate of temperature rate of change.

### 2.2.1 Salt Lake City airport

Figure 1 illustrates the historical maximum and minimum annual average temperatures recorded from 1948 through 2006, at the weather station located at the Salt Lake City airport (data available at <http://www.wrcc.dri.edu/cgi-bin/cliMAIN.pl?ut7598>; WRCC, 2006d).

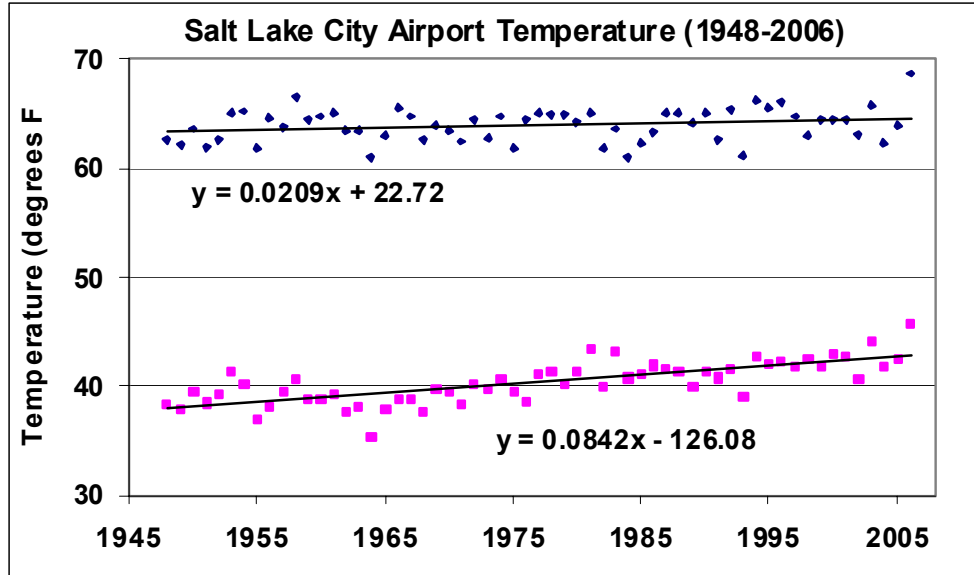


**Figure 1. Maximum and minimum annual temperatures (in °F) at the Salt Lake City airport from 1948 through 2006.**

Using the 90% confidence interval, trends indicate that:

- ▶ Maximum temperatures are increasing at a rate of  $0.2^{\circ}\text{F}/\text{decade} \pm 0.19^{\circ}\text{F}$ . This implies a range of temperature warming from  $0.01^{\circ}\text{F}/\text{decade}$  to  $0.39^{\circ}\text{F}/\text{decade}$ .
- ▶ Minimum temperatures are warming more rapidly at a rate of  $0.84^{\circ}\text{F}/\text{decade} \pm 0.16^{\circ}\text{F}$ . This implies a range of temperature warming from  $0.68^{\circ}\text{F}/\text{decade}$  to  $1.0^{\circ}\text{F}/\text{decade}$ .

Figure 2 illustrates the historical maximum and minimum annual average temperatures recorded from 1970 through 2006, at the weather station located at the Salt Lake City airport.

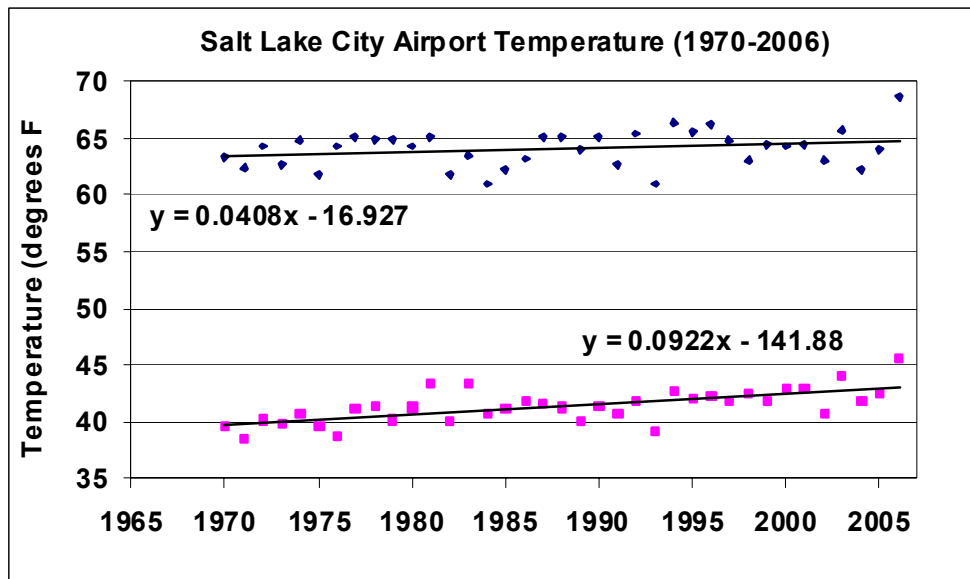


**Figure 2. Maximum and minimum annual temperatures (in  $^{\circ}\text{F}$ ) at the Salt Lake City airport from 1970 through 2006.**

Using the 90% confidence interval, trends indicate that:

- ▶ Maximum temperatures from 1970 to 2006 are increasing at a rate of  $0.41^{\circ}\text{F}/\text{decade} \pm 0.4^{\circ}\text{F}$ . This implies a range of temperature warming from  $0.01^{\circ}\text{F}/\text{decade}$  to  $0.81^{\circ}\text{F}/\text{decade}$ .
- ▶ Minimum temperatures are warming more rapidly at a rate of  $0.92^{\circ}\text{F}/\text{decade} \pm 0.3^{\circ}\text{F}$ . This implies a range of temperature warming from  $0.62^{\circ}\text{F}/\text{decade}$  to  $1.2^{\circ}\text{F}/\text{decade}$ .

### 2.2.2 Solitude/Brighton

Figure 3 illustrates the historical maximum and minimum annual average temperatures recorded from 1949 through 2005, at the weather station located at Solitude Brighton (data available at <http://www.wrcc.dri.edu/cgi-bin/cliMAIN.pl?ut7846>; WRCC, 2006e).

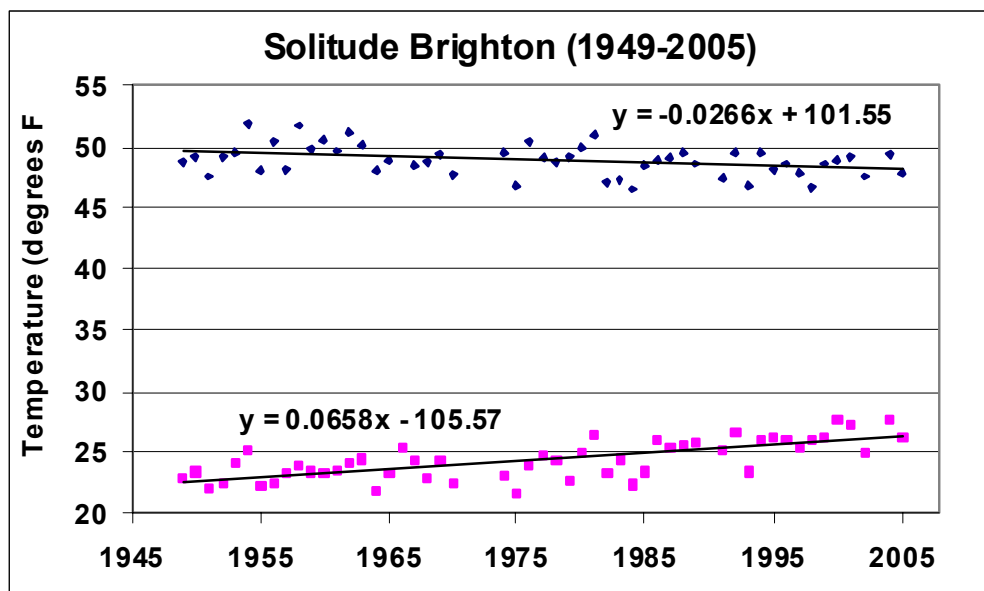


**Figure 3. Maximum and minimum annual temperatures (in °F) at the Solitude Brighton weather station from 1949 through 2005.**

Using the 90% confidence interval, trends indicate that:

- ▶ Maximum temperatures are *decreasing* at a rate of  $0.26^{\circ}\text{F}/\text{decade} \pm 0.16^{\circ}\text{F}$ . This implies a range of temperature *cooling* from  $-0.42^{\circ}\text{F}/\text{decade}$  to  $-0.1^{\circ}\text{F}/\text{decade}$ .
- ▶ Minimum temperatures are warming at a rate of  $0.66^{\circ}\text{F}/\text{decade} \pm 0.16^{\circ}\text{F}$ . This implies a range of temperature warming from  $0.5^{\circ}\text{F}/\text{decade}$  to  $0.81^{\circ}\text{F}/\text{decade}$ .

Figure 4 illustrates the historical maximum and minimum annual average temperatures recorded over the last quarter century only (1970 through 2005), at the weather station located at Solitude Brighton.

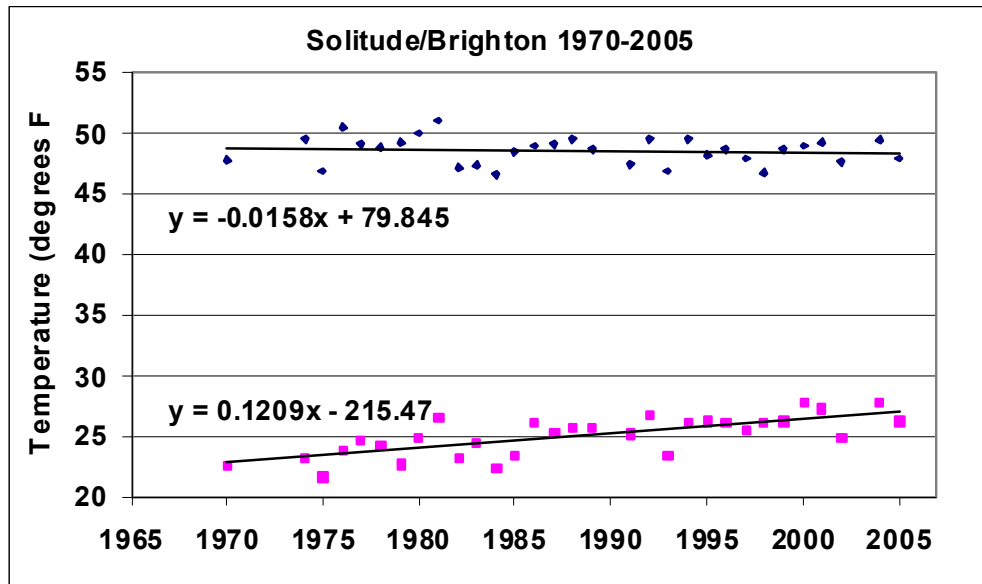


**Figure 4. Maximum and minimum annual temperatures (in °F) at the Solitude Brighton weather station from 1970 through 2005.**

Using the 90% confidence interval, trends indicate that:

- ▶ Maximum temperatures display no discernable trend, with a range of temperature changes from  $-0.5^{\circ}\text{F}/\text{decade}$  to  $0.2^{\circ}\text{F}/\text{decade}$ .
- ▶ Minimum temperatures are warming at a rate of  $1.2^{\circ}\text{F}/\text{decade} \pm 0.35^{\circ}\text{F}$ . This implies a range of temperature warming from  $0.86^{\circ}\text{F}/\text{decade}$  to  $1.56^{\circ}\text{F}/\text{decade}$ .

### 2.2.3 Logan

Figure 5 illustrates the historical maximum and minimum annual average temperatures recorded from 1896 through 2006, at the weather station located at Utah State University in Logan (data available at <http://www.wrcc.dri.edu/cgi-bin/cliMAIN.pl?ut5186>; WRCC, 2006b).

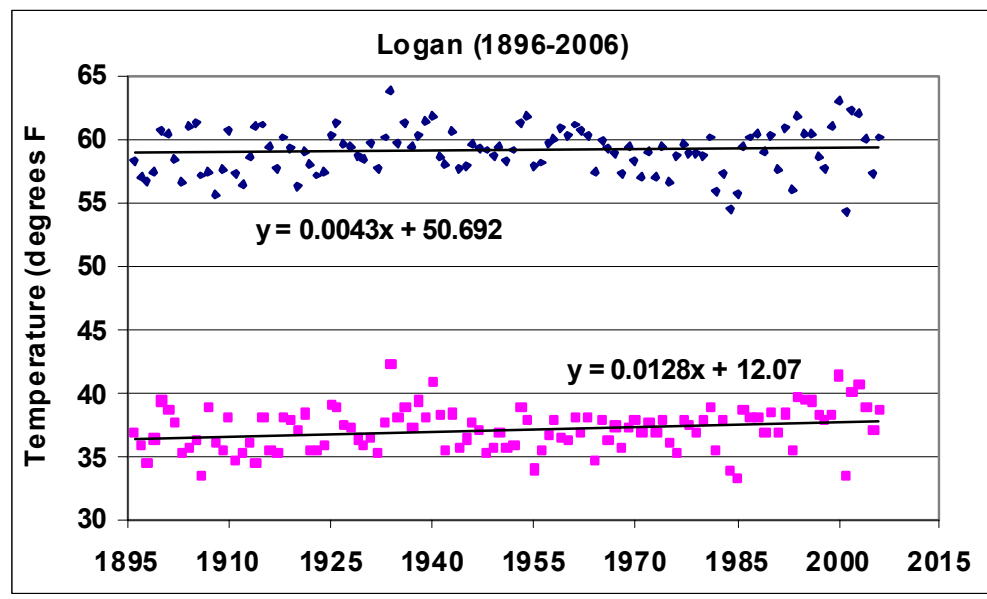


**Figure 5. Maximum and minimum annual temperatures (in °F) at the Utah State University weather station in Logan from 1896 through 2006.**

Using the 90% confidence interval, trends indicate that:

- ▶ Maximum temperatures display no discernable trend, with a range of temperature changes from  $-0.045^{\circ}\text{F}/\text{decade}$  to  $0.13^{\circ}\text{F}/\text{decade}$ .
- ▶ Minimum temperatures are warming at a rate of  $0.13^{\circ}\text{F}/\text{decade} \pm 0.08^{\circ}\text{F}$ . This implies a range of temperature warming from  $0.05^{\circ}\text{F}/\text{decade}$  to  $0.21^{\circ}\text{F}/\text{decade}$ .

Figure 6 illustrates the historical maximum and minimum annual average temperatures recorded over the last quarter century only (1970 through 2006), at the weather station located at Utah State University in Logan.

Using the 90% confidence interval, trends indicate that:

- ▶ Maximum temperatures are increasing at a rate of  $0.63^{\circ}\text{F}/\text{decade} \pm 0.52^{\circ}\text{F}$ . This implies a range of temperature increases from  $0.1^{\circ}\text{F}/\text{decade}$  to  $1.15^{\circ}\text{F}/\text{decade}$ .
- ▶ Minimum temperatures are warming at a rate of  $0.57^{\circ}\text{F}/\text{decade} \pm 0.45^{\circ}\text{F}$ . This implies a range of temperature warming from  $0.1^{\circ}\text{F}/\text{decade}$  to  $1.0^{\circ}\text{F}/\text{decade}$ .

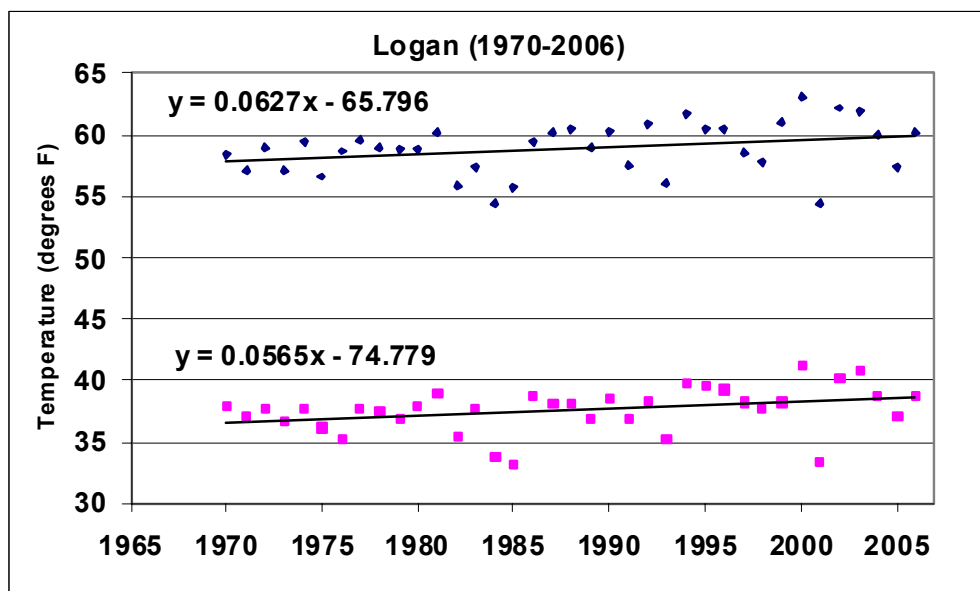


**Figure 6. Maximum and minimum annual temperatures (in °F) at the Utah State University weather station in Logan from 1970 through 2006.**

#### 2.2.4 Mountain Dell Dam

Figure 7 illustrates the historical maximum and minimum annual average temperatures recorded from 1949 through 2005, at the weather station located at the Mountain Dell Dam (data available at <http://www.wrcc.dri.edu/cgi-bin/cliMAIN.pl?ut5892>; WRCC, 2006c).

Using the 90% confidence interval, trends indicate that:

- ▶ Maximum temperatures display no discernable trend, with a range of temperature changes from  $-0.25^{\circ}\text{F}/\text{decade}$  to  $0.3^{\circ}\text{F}/\text{decade}$ .
- ▶ Minimum temperatures are warming at a rate of  $0.73^{\circ}\text{F}/\text{decade} \pm 0.2^{\circ}\text{F}$ . This implies a range of temperature warming from  $0.53^{\circ}\text{F}/\text{decade}$  to  $0.93^{\circ}\text{F}/\text{decade}$ .

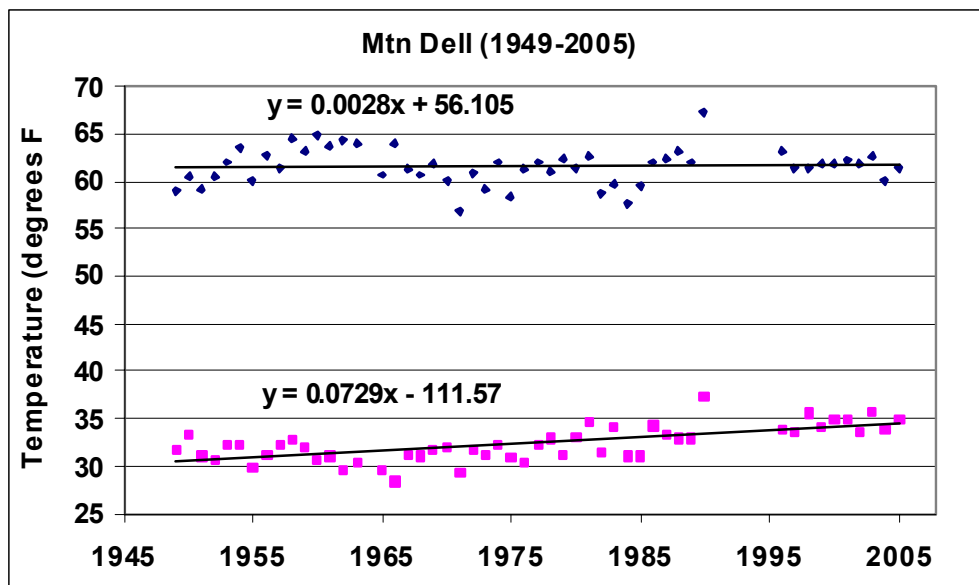


**Figure 7. Maximum and minimum annual temperatures (in °F) at the Mountain Dell Dam weather station from 1949 through 2005.**

Figure 8 illustrates the historical maximum and minimum annual average temperatures recorded over the last quarter century only (1970 through 2005), at the weather station located at the Mountain Dell Dam.

Using the 90% confidence interval, trends indicate that:

- ▶ Maximum temperatures are increasing at a rate of  $0.66^{\circ}\text{F}/\text{decade} \pm 0.5^{\circ}\text{F}$ . This implies a range of temperature increases from  $0.16^{\circ}\text{F}/\text{decade}$  to  $1.16^{\circ}\text{F}/\text{decade}$ .
- ▶ Minimum temperatures are warming at a rate of  $1.15^{\circ}\text{F}/\text{decade} \pm 0.36^{\circ}\text{F}$ . This implies a range of temperature warming from  $0.8^{\circ}\text{F}/\text{decade}$  to  $1.5^{\circ}\text{F}/\text{decade}$ .

### 2.2.5 Alta station

Figure 9 displays maximum and minimum annual average temperatures from the weather station located at Alta from 1970 through 2006 (data available at <http://www.wrcc.dri.edu/cgi-bin/cliMAIN.pl?ut0072>; WRCC, 2006a). The abrupt change in 1970 could be due to one of several factors: the station may have been moved, the instruments may have changed, observation techniques may have changed, or a combination of these factors. Therefore, only post-1970 is evaluated here.

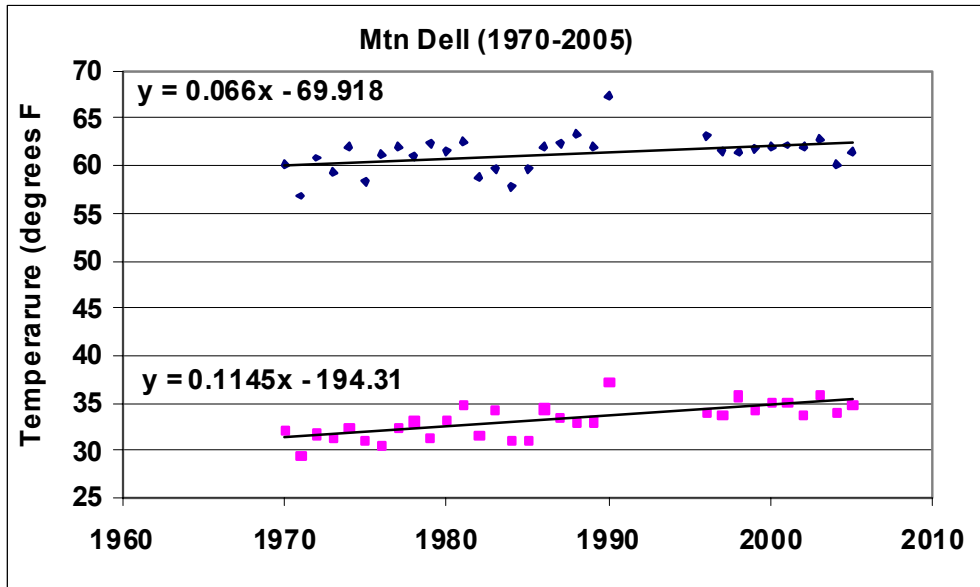


Figure 8. Maximum and minimum annual temperatures (in °F) at the Mountain Dell Dam weather station from 1970 through 2005.

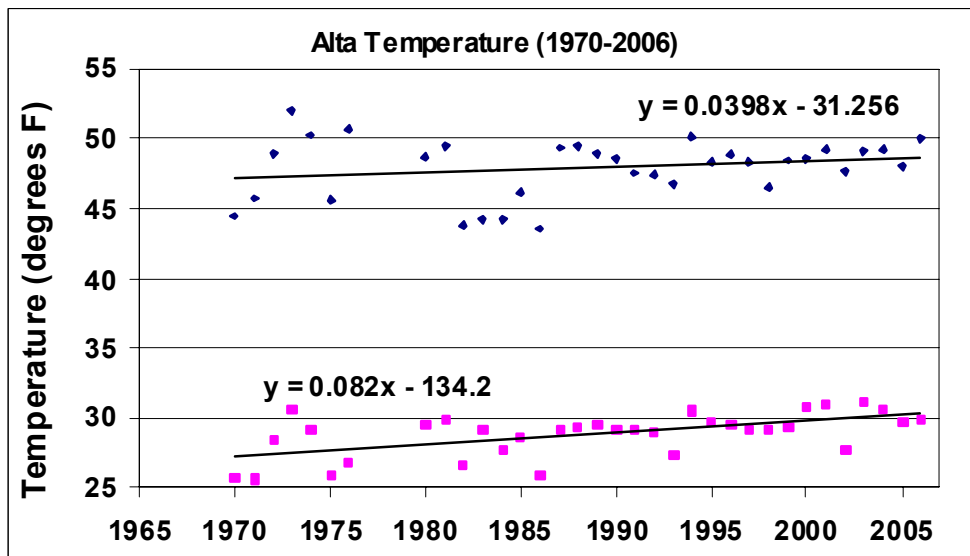


Figure 9. Maximum and minimum annual temperatures (in °F) at the Alta weather station from 1970 through 2006.

Using the 90% confidence interval, trends indicate that:

- ▶ Maximum temperatures show no discernible trend, with a range of temperature changes from  $-0.17^{\circ}\text{F}/\text{decade}$  to  $0.97^{\circ}\text{F}/\text{decade}$ .
- ▶ Minimum temperatures are warming at a rate of  $0.82^{\circ}\text{F}/\text{decade} \pm 0.35^{\circ}\text{F}$ . This implies a range of temperature warming from  $0.47^{\circ}\text{F}/\text{decade}$  to  $1.2^{\circ}\text{F}/\text{decade}$ .

### 2.2.6 Summary of temperature trends

Tables 1 and 2 summarize the trend analysis results, using the 90% confidence interval. The temperature ranges indicate the lower and upper bounds of temperature change per decade.

**Table 1. Summary of temperature trends using the entire available temperature record (full records)**

Weather station	Max. temp range (°F)	Min. temp range (°F)	Period of record
Salt Lake City airport	0.02 to 0.4	0.68 to 1.0	1948 to 2006
Solitude/Brighton	-0.42 to -0.1	0.5 to 0.81	1949 to 2005
Logan	-0.04 to 0.13	0.05 to 0.21	1896 to 2006
Mountain Dell	-0.25 to 0.3	0.53 to 0.93	1949 to 2005

**Table 2. Summary of temperature trends using only post-1970 data (1970 through 2006)**

Weather station	Max. temp range (°F)	Min. temp range (°F)
Salt Lake City airport	0.004 to 0.81	0.62 to 1.2
Alta	-0.17 to 0.97	0.47 to 1.2
Solitude/Brighton	-0.5 to 0.2	0.86 to 1.6
Logan	0.1 to 1.15	0.1 to 1.0
Mountain Dell <sup>a</sup>	0.15 to 1.17	0.8 to 1.5

a. Data through 2005 only.

From the above temperature trends, we can draw the following conclusions:

1. Daily minimum temperatures are warming faster than daily maximum temperatures in all locations.
2. Minimum temperatures are warming between 0.05° and 1.6°F per decade. This implies that a 5°F warming could be reached by mid-century. This finding is consistent with the climate model projections we discuss in Section 2.6.
3. It is uncertain whether or not maximum daily temperatures are warming, cooling, or staying the same. The temperature *change* ranges from -0.5° to 1.17°F per decade. This is consistent with IPCC projections that minimum temperatures are likely to be more affected than maximum temperatures.
4. Warming trends are more pronounced after 1970, as compared to the entire available historical record.

## 2.3 Future Climate Change Scenarios

While some aspects of change, such as increased temperature, are quite likely, other aspects are uncertain. For example, although temperatures will eventually rise in most regions of the world, the direction of change in many other key variables, such as precipitation, are uncertain for most regions.<sup>7</sup> Even where the direction of change is certain or likely, there is uncertainty about the magnitude and path of change.

To capture the range of uncertainty in the future climate, we developed scenarios of plausible combinations of conditions that represent possible future situations. Scenarios are often used to assess the consequences of possible future conditions, and how organizations or individuals might prepare for and respond to them. For example, businesses might use scenarios of future economic conditions to decide whether certain strategies or investments make sense now.

The scenarios that we used bracket a plausible range of potential changes in climate. By evaluating a range of plausible conditions, we were able to improve our understanding of the sensitivity at a local scale to the potential changes.

We developed scenarios for three periods: the 2030s, 2070s, and the 2100s. These time periods are not selected to predict weather in a particular future year, but to estimate how average climate conditions may change. We project out to 2100 because it is likely that the current path

---

7. Other anthropogenic activities such as land use changes and air pollutant emissions can have as significant an impact on local and regional climate change as the influence of increased GHG concentrations.

of GHG emissions will lead to substantial changes in climate at least that far into the future (although reduction of emissions could substantially reduce climate change over this century). For the remainder of the report we will refer to these time periods as the years 2030, 2075, and 2100.

## 2.4 Selecting Climate Change Scenarios

Three factors are critical for modeling how Park City's climate might change:

1. GHG emissions
2. Sensitivity of global climate to increases in GHG concentrations
3. Patterns of regional climate change.

Estimates of GHG emissions and the sensitivity of GMT to increases in GHG concentrations are inputs to the models we used to project changes in climate variables. We then examined the projections of several climate models for a single region to explore projected patterns of regional climate change. We describe GHG emissions scenarios and the issue of a climate sensitivity parameter in the sections that follow.

### 2.4.1 GHG emissions

Future changes in GHG emissions depend on many factors, including population growth, economic growth, technology, government, and society. The IPCC tried to capture a wide range of potential changes in GHG emissions in its *Special Report on Emission Scenarios* (SRES; (Nakićenović and Swart, 2000). The seven scenarios that IPCC developed reflect very different conditions regarding population growth, economic growth, how even the growth is across the world, the level of economic integration, the strength of environmentalism, and improvements in technology. To estimate potential future changes for Park City, we used IPCC scenarios that represent a range of potential future GHG emissions and concentrations. For most of our evaluations, we used B1 as the low-end projection, A1FI as the high-end projection, and A1B as a mid-range projection. For one of our modeling approaches, we used B2 as a moderate projection, and A2 as a high projection.

Figure 10(a) shows emissions for all seven of the SRES scenarios. CO<sub>2</sub> is one of the GHGs that contributes to climate change, and we show it here as an illustration of the total GHG emissions modeled in each of the scenarios. Compared to current CO<sub>2</sub> emissions of 7 gigatons (Gt)/year, A1B reaches 15 Gt/year by 2030, peaks at about 17 Gt/year by 2050, and slightly declines to about 13 Gt/year by 2100. The A1FI scenario has slightly higher CO<sub>2</sub> emissions than A1B by 2030, but by 2050 is at 24 Gt/year, and by 2080 reaches 29 Gt/year. From there, the emissions

slightly decrease. In contrast, the B1 scenario emits 9 Gt/year by 2030, peaks at 10 Gt/year in 2040, and then declines to 6 Gt/year in 2100.

Figure 10(b) shows atmospheric CO<sub>2</sub> concentrations projected to result from the emissions scenarios. For thousands of years before the Industrial Revolution, CO<sub>2</sub> concentrations were around 280 parts per million (ppm). Today, concentrations have increased to about 380 ppm. For the 2030s, CO<sub>2</sub> concentrations across all SRES scenarios are similar, even though there are projected to be substantial differences in CO<sub>2</sub> emissions [Figure 10(a)]. According to the TAR, however, there are substantial differences in aerosol emissions that can have significant impacts on regional climate. By 2050, the CO<sub>2</sub> concentrations projected by the seven scenarios begin to diverge, and by 2100, there is a wide spread in estimated concentrations. Scenario A1B is approximately in the middle of the range of projected future concentrations, reaching close to 700 ppm by 2100. A1FI has the highest concentrations, reaching over 900 ppm by 2100, and B1 has the lowest, reaching just over 500 ppm by 2100. The A2 scenario produces CO<sub>2</sub> concentrations of about 850 ppm by 2100, which is between A1B and A1FI. The B2 scenario produces CO<sub>2</sub> concentrations of about 600 ppm by 2100, which is between A1B and B1.

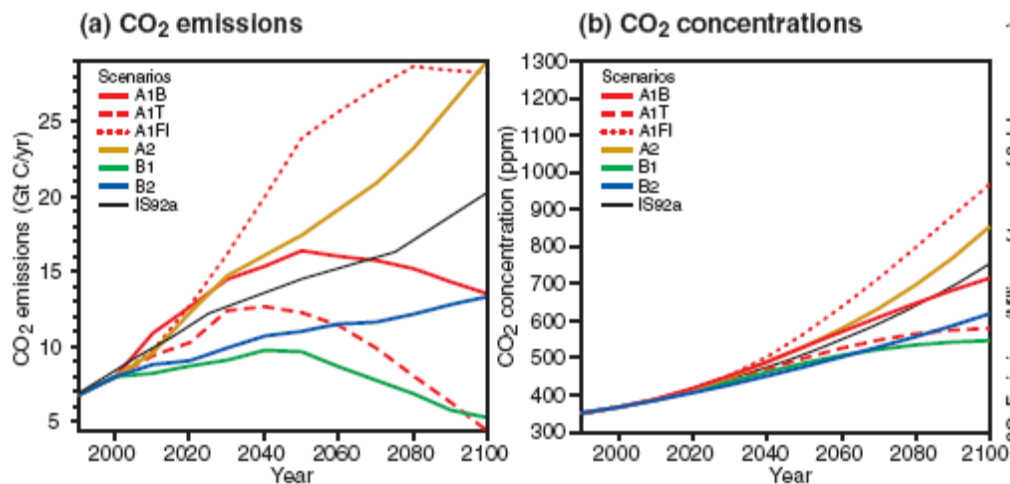


**Figure 10. SRES projections of CO<sub>2</sub> emissions and concentrations.**

In addition to representing low, middle, and high projections for GHG emissions and concentrations, scenarios B1, A1B, and A1FI represent the low, middle, and high projections for GMT. In 2030, we only used A1B since the three scenarios are so similar at that time, but for 2075 and 2100 projections, we used all three. The A1B has very high sulfur dioxide (SO<sub>2</sub>) emissions early in the century. Since sulfate emissions can result in decreased precipitation in the Rockies (Borys et al., 2003), this scenario would have a substantial impact on precipitation over the Rockies.

The A1, A2, B1, and B2 IPCC scenarios are described in more detail in Appendix A.

### 2.4.2 Sensitivity

The second critical factor affecting projections of the effect on increasing concentrations of GHGs on climate in Park City is how much the Earth's climate will warm for a given increase in CO<sub>2</sub> concentration in the atmosphere. This relationship is not well described. Factors such as how cloud cover will change and how various feedback from the Earth will affect warming are not well characterized. To project future climate though, we must parameterize the models with a sensitivity estimate. Typically, sensitivity is expressed as the rise in GMT as a result of a doubling of the atmospheric CO<sub>2</sub> concentration ( $2 \times \text{CO}_2$ ). Based on a recent review of sensitivity (Kerr, 2004)<sup>8</sup> and consultations with several atmospheric scientists, we decided to use 3°C as the estimate of sensitivity.

## 2.5 Climate Models

We used three types of modeling approaches to examine potential future climate:

- ▶ MAGICC/SCENGEN, which is a coupling of two models that allow users to investigate future climate change and its uncertainties at regional scales (Wigley, 2004). MAGICC stands for Model for the Assessment of Greenhouse-gas Induced Climate Change. SCENGEN stands for Global and Regional Climate SCENario GENERator.
- ▶ PCM-RCM, which is a high-resolution RCM built for a region such as the United States, that is “nested” within a GCM. We used an RCM called MM5 (Leung et al., 2003a, 2003b, 2004; Leung and Qian, 2005), that is nested in the PCM (Dai et al., 2004).
- ▶ SDSM, in which we use the statistical relationship between variables at a large scale and at a local scale to estimate how climate at a specific location, such as a weather station, may change in response to changes in GHG concentrations.

---

8. Kerr (2004) notes that there is confidence among climate modelers that the  $2 \times \text{CO}_2$  sensitivity (i.e., the increase in GMT due to a doubling of CO<sub>2</sub>) is at least 1.5°C. The most likely sensitivity is between 2.5° and 3°C. Kerr reports that the most probable sensitivity is 3°C. There is substantial uncertainty about the upper end of the range. A number of studies such as Forest et al. (2002) and Andronova and Schlesinger (2001) find that there is a 10% chance the upper end of the range is as high as 7° to 9°C.

### 2.5.1 MAGICC/SCENGEN

MAGICC uses GHG emissions scenarios to project global-mean temperature and sea level change. SCENGEN constructs climate change scenarios using results from MAGICC, and scales the results to project regional climate changes in 5° latitude by 5° longitude cells (approximately 300 miles on a side). Output from SCENGEN includes changes in temperature and precipitation and changes in temperature and precipitation variation.

The SCENGEN grid boxes around Park City are shown in Figure 11. In reality, climate within a grid box can vary substantially because of topographic relief. SCENGEN does not capture climatic differences within grid boxes. For this study, we examined projections for the grid box in which Park City lies and the adjacent grid box to the south because Park City is close to the southern edge of its grid box.

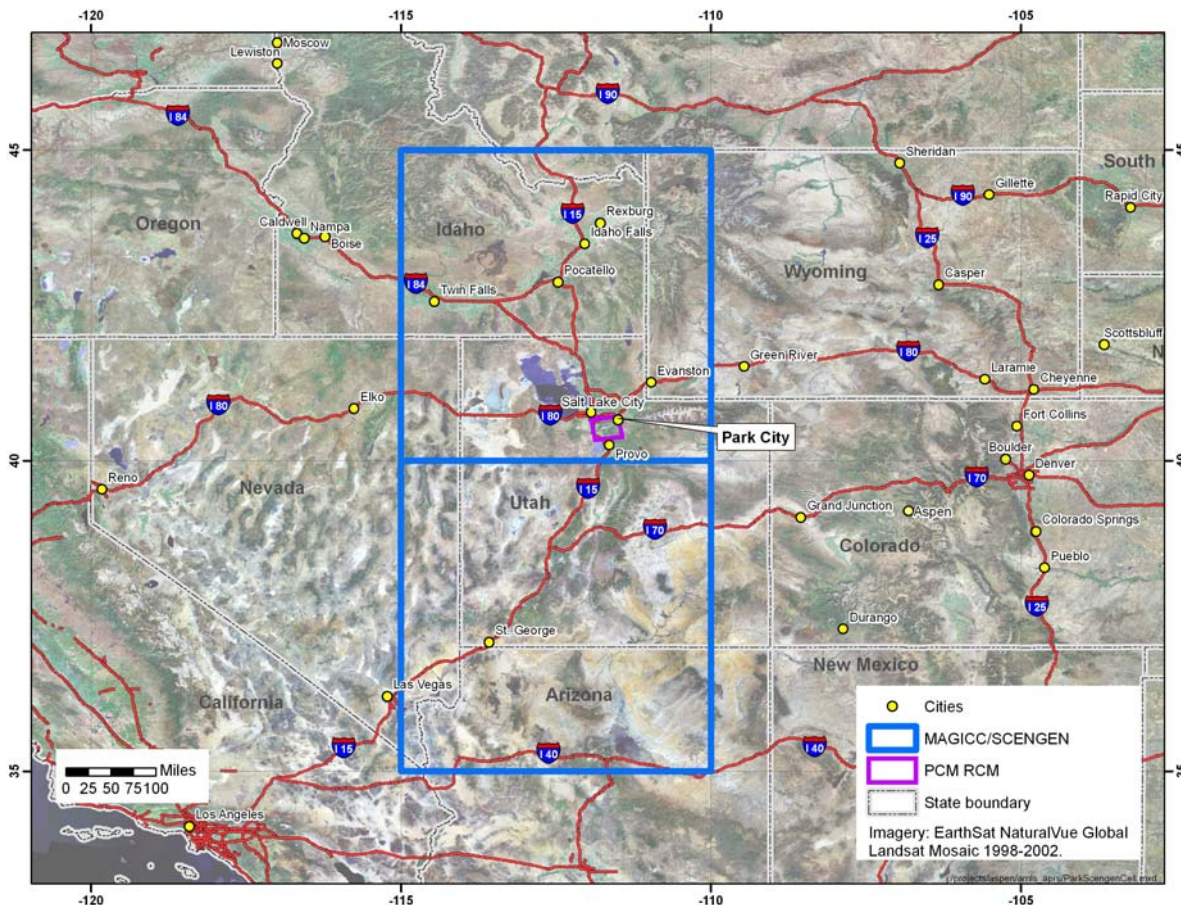


**Figure 11. SCENGEN grid boxes and PCM-RCM domain containing Park City.** The coordinates of the boxes are 35° to 45°N latitude and 110° to 115°W longitude.

To run MAGICC/SCENGEN, the user must define which GCMs to include as climate drivers. GCMs are sophisticated, complex models that form the basis for many climate change models. GCMs attempt to mimic the Earth's climate drivers, including the oceans, land, ice, the atmosphere, and the biosphere, by integrating equations of fluid dynamics, chemistry, and biology.

There are numerous GCMs. We were most interested in models that simulate well the climate over the central Rocky Mountains. In an evaluation of the ability of 17 existing GCMs to simulate current climate in western North America, Wigley (2006) concluded that the following five models performed best:

- ▶ CSIRO – Commonwealth Scientific and Industrial Research Organisation, Australia
- ▶ ECHAM3 – Max Planck Institute for Meteorology, Germany
- ▶ ECHAM4 – Max Planck Institute for Meteorology, Germany
- ▶ HadCM2 – Hadley Model, United Kingdom Meteorological Office
- ▶ HadCM3 – Hadley Model, United Kingdom Meteorological Office.

We examined climate projections from MAGICC/SCENGEN using each of the five GCMs independently, and using an average of output from the five GCMs. Appendix B presents an analysis of the five models' simulation of current climate in the two SCENGEN grid boxes.

### 2.5.2 PCM-RCM

For a higher resolution estimate of changes in climate in the Park City area, we examined output from PCM-RCM. We used output for the approximately 36 km (20 mile) grid box containing Park City. The approximate boundaries of the PCM-RCM grid box are 40.33° to 40.71°N to 111.50° to 111.87°W. The average elevation of the grid box is 2,086 m (6,844 ft). The PCM RCM projected results for the selected years are averages of time periods centered on the specific years. The time periods are defined as follows: 2030 is the average of model simulations for 2020 to 2040, and 2070 is the average of model simulations for 2065 to 2075. The projected changes in precipitation and temperature are reported as changes relative to the base period of 1985 (the average of model simulations for 1976 to 1995). We used the temperature and precipitation outputs from PCM-RCM for the snowpack analysis.

### 2.5.3 SDSM

The statistical relationship between climate variables at a large scale and at a local scale can be used to estimate how climate at a specific location may change as a result of the GCM projections for climate change. This approach assumes that the current relationship between climate variables at a large-scale and at a specific location do not vary with climate change. The

assumption could be wrong, but nonetheless, the approach can be used to develop a scenario for a specific location.

The only emissions scenarios that can be downscaled are A2 and B2. We used these emissions scenarios and output from the HadCM3 GCM for the grid cell containing Park City. The output was downscaled using the SDSM to the Thaynes Canyon SNOpack TELelemetry (SNOTEL) weather station (NRCS, 2006) at the mid-mountain station at the Park City ski area (R. Wilby, Appendix C).

## 2.6 Projections of Climate Change

### 2.6.1 MAGICC/SCENGEN

We first report temperature and precipitation projections for the central A1B emission scenario for each of the five individual GCMs and for the average of the five GCMs in 2030, 2075, and 2100. We then examine the differences between temperature and precipitation projected for each of the three emissions scenarios (A1FI, A1B, and B1), using the average of the five GCMs as input to MAGICC/SCENGEN.

Figure 12(A) presents estimated change in annual temperature (in °C) for Park City in 2030 (relative to 1990) using the A1B scenario. The first five bars are results for individual models; the last bar is the model average. Under this scenario, the average model warming is 2°C (about 4°F), with a range of 1.8° to 2.2°C (3° to 4°F), and little variability across the GCMs.

Figure 12(B) presents the estimated changes in precipitation in 2030 relative to 1900 for A1B. Four of the five GCMs project a decrease in precipitation for Park City. HadCM2 projects a slight increase. The GCM average projects a 7% decrease. The projected changes in precipitation range from -16.2% to 1.3%. Estimated decreases are partially a result of the assumed increase in GHGs and partially the result of aerosols (e.g., SO<sub>2</sub>). If aerosol increases are not as large as in the A1B scenario, estimated decreases in precipitation would not be as large.

By 2075, average warming near Park City for the A1B scenario is 4.9°C (8.8°F) with a range of 4.4° to 5.2°C (7.9° to 9.4°F). All five GCMs project similar results (Figure 13A). Projections for precipitation are much more variable: the projected changes in precipitation range from -32.5% to 4.4% (Figure 13B). The average projected precipitation is a decrease of 14.3%. Again, HadCM2 is the only one of the five GCMs that projects an increase in precipitation.

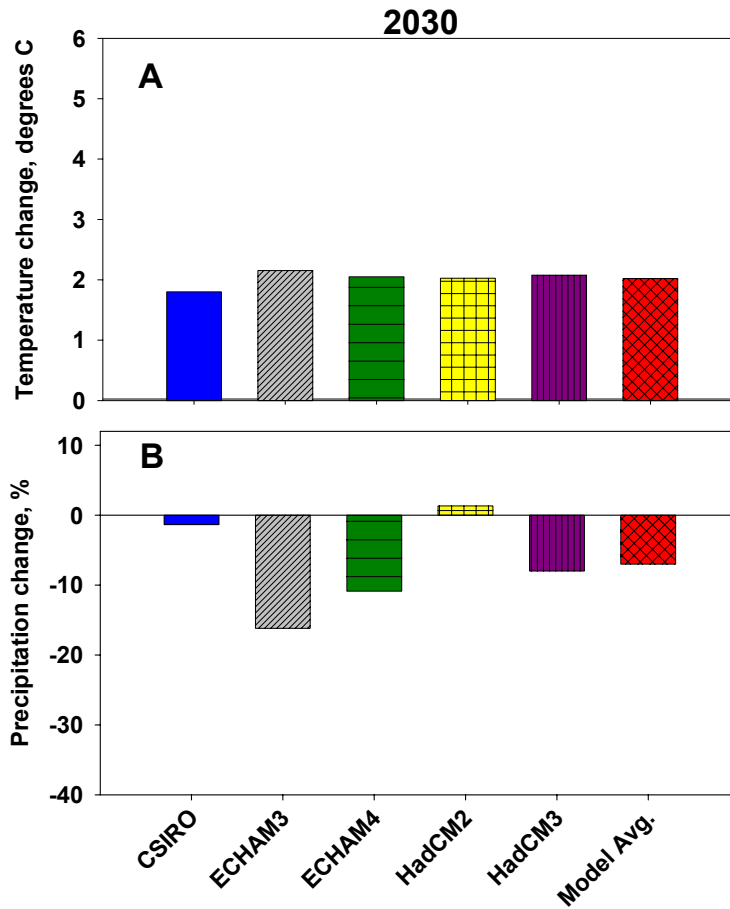


Figure 12. Estimated annual temperature (A) and precipitation (B) changes in Park City, predicted by five GCMs, for the A1B emission scenario in 2030.

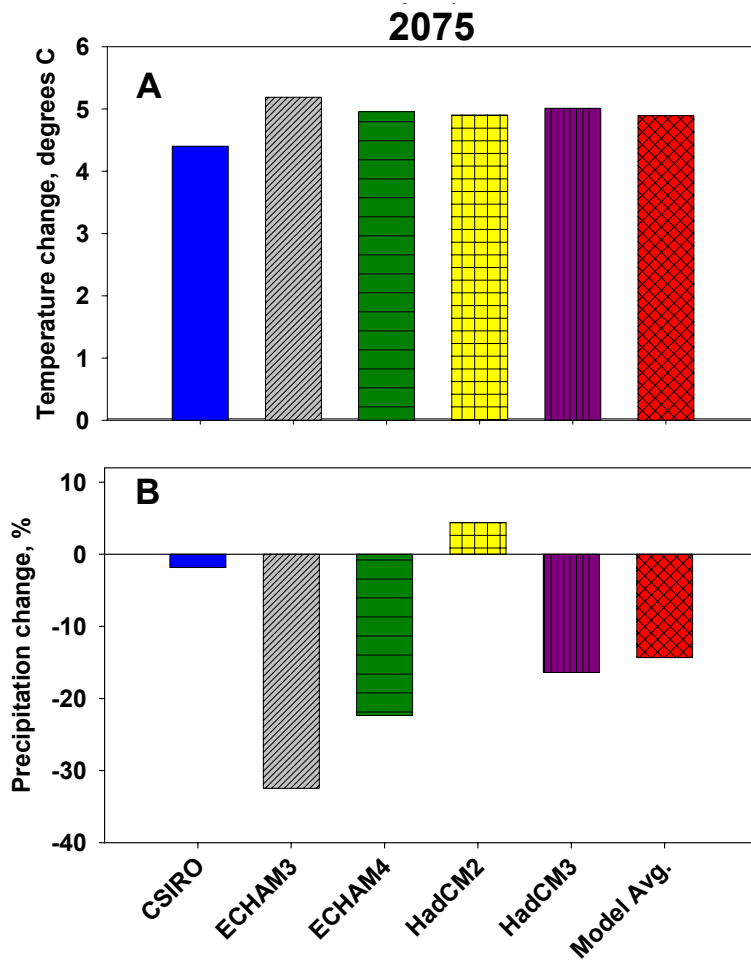
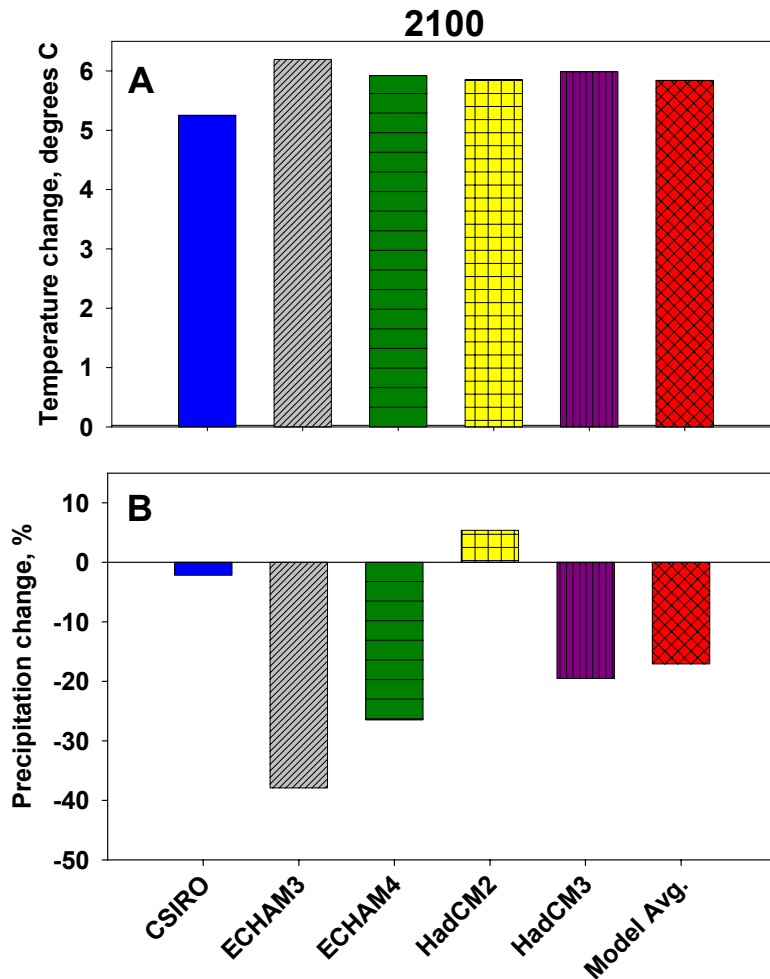


Figure 13. Estimated annual temperature (A) and precipitation (B) changes in Park City, predicted by five GCMs, for the A1B emission scenario in 2075.

By 2100, the five GCMs project an average warming near Park City of 5.8°C (10.4°F), with a range of 5.3° to 6.2°C (9.5° to 11.6°F) (Figure 14A). The average of the five GCMs projects a precipitation decrease by 17.1% compared to 1990 (Figure 14B). The wettest model, HadCM2, projects a 5.4% increase in precipitation, while the driest, ECHAM3, projects a 37.9% decrease.



**Figure 14. Estimated annual temperature (A) and precipitation (B) changes in Park City, predicted by five GCMs, for the A1B emission scenario in 2100.**

Even though four of the five models project a decrease in precipitation, we do not interpret this as a consensus. There is too much variability across the models to be confident about whether precipitation will increase or decrease.

We next examined differences between temperature and precipitation projected for each of the three emissions scenarios (B1 – low, A1B – middle, and A1FI – high) in 2030, 2075, and 2100, using the average of the five GCMs as input to MAGICC/SCENGEN (Tables 3 and 4). The temperature projections increase with increasing GHG emissions, and with time. Under the high GHG emissions scenario (A1FI), the average temperature increase in 2075 is 6.3°C (11.3°F), and in 2100 is 8.4°C (15.1°F). Under the low GHG emissions scenario (B1), the average temperature increase is 4.2°C (7.6°F) in 2075 and 4.7°C (8.5°F) in 2100. The largest temperature increases are projected for the summer months, while the smallest increases are projected for the winter months. This is the case for all three emissions scenarios (Figure 15).

**Table 3. MAGICC/SCENGEN projections of mean annual temperature change (°C) relative to 1990 for low, middle, and high emissions scenarios.** “Average” = averaged input from five GCMs. “Range” = range of results from each of the five individual GCMs.

Year	Emissions scenario					
	B1 – low		A1B – middle		A1FI – high	
	Average	Range	Average	Range	Average	Range
2030	1.7	1.5 to 1.8	2	1.8 to 2.2	1.9	1.6 to 2
2075	4.2	3.8 to 4.4	4.9	4.4 to 5.2	6.3	5.6 to 6.7
2100	4.7	4.2 to 4.9	5.8	5.3 to 6.2	8.4	7.4 to 8.9

**Table 4. MAGICC/SCENGEN projections of mean annual precipitation change (%) relative to 1990 for low, middle, and high emissions scenarios, using averaged input from five GCMs.** “Average” = averaged input from five GCMs. “Range” = range of results from each of the five individual GCMs.

Year	Scenarios					
	B1 – low		A1B – middle		A1FI – high	
	Average	Range	Average	Range	Average	Range
2030	-6.8	-15 to 0.6	-7	-16.2 to 1.3	-6.8	-15.8 to 1.4
2075	-13.7	-28.9 to 1.3	-14.3	-32.5 to 4.4	-16.8	-40.2 to 9.7
2100	-15.5	-31.9 to 0.9	-17.1	-37.9 to 5.4	-20.8	-49.3 to 15.0

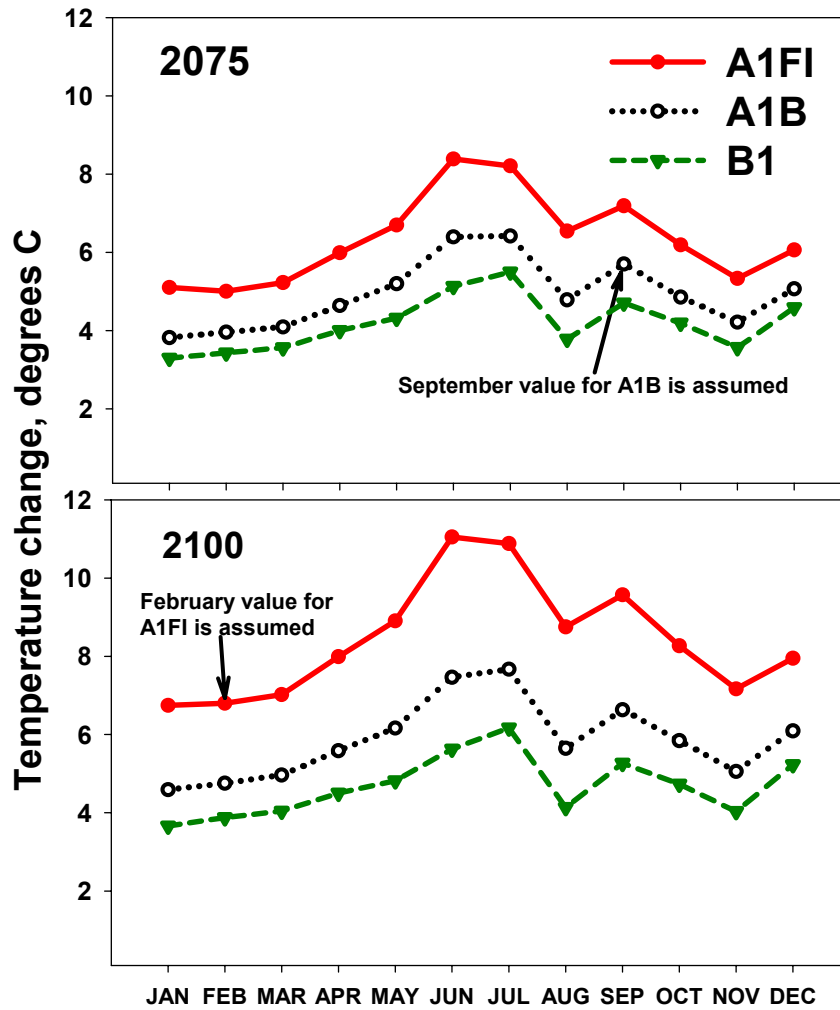
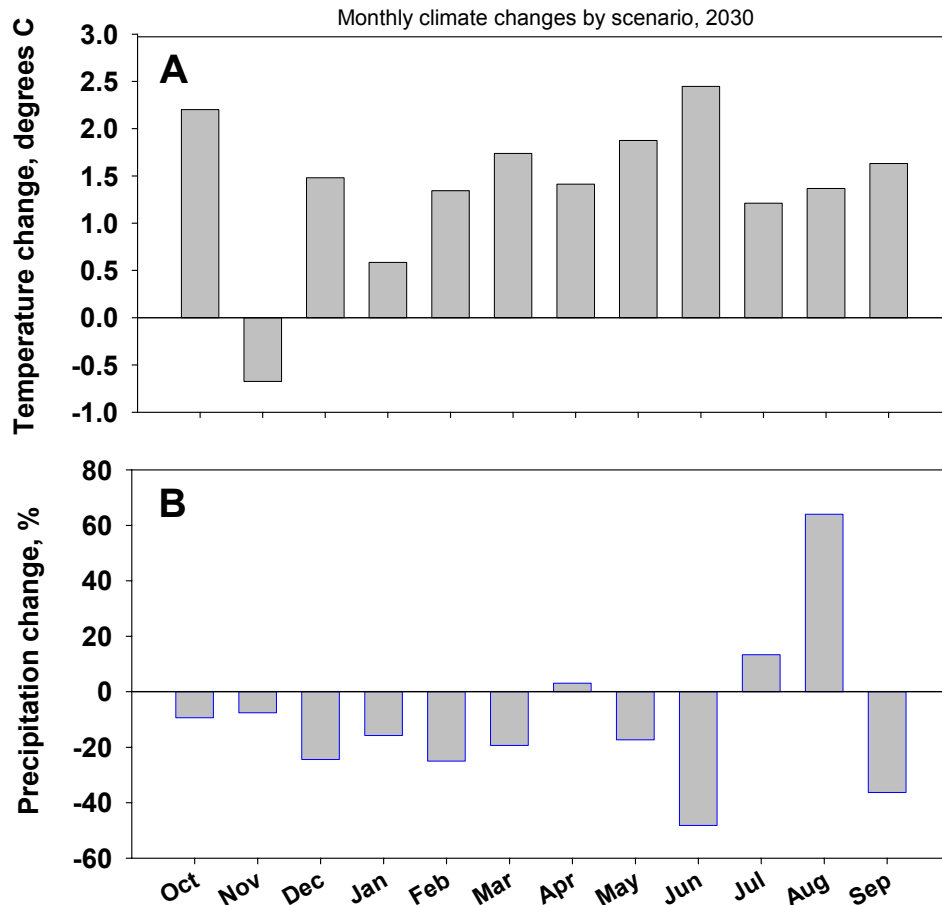


Figure 15. MAGICC/SCENGEN projections of monthly average temperature changes for the A1FI – high, A1B – middle, and B1 – low emission scenarios for 2075 and 2100, using averaged projections from five GCMs as input.

The projected average decrease in precipitation also becomes more extreme with increasing GHG emissions, and with time. The range of change in precipitation appears to be more sensitive to the choice of GCM than to emissions scenario (Table 4). Predictions of the change in precipitation are more uncertain than predictions of the change in temperature.

**2.6.2 PCM-RCM**

For the Park City area in 2030, PCM-RCM projects an increase in temperature relative to the base year 1985, for each month except November (Figure 16A). Averaged over the year, precipitation is projected to change by less than 10%. However, PCM-RCM projects a decrease in precipitation from October through March, and an increase in April, July, and August (Figure 16B).



**Figure 16. Projected changes in monthly average temperature (A) and precipitation (B) from PCM-RCM in 2030.**

By 2070,<sup>9</sup> the average annual temperature increase is greater than that estimated for 2030, and most monthly average temperature increases are greater than in 2030 (Figure 17A). In January, temperature is projected to decrease relative to 1985. Average annual precipitation is projected to decrease by approximately 10%. This annual decrease is caused by a projected 40% decrease for May through September (Figure 17B). Precipitation in October through April is projected to increase by 6% despite February being projected to be 40% drier.

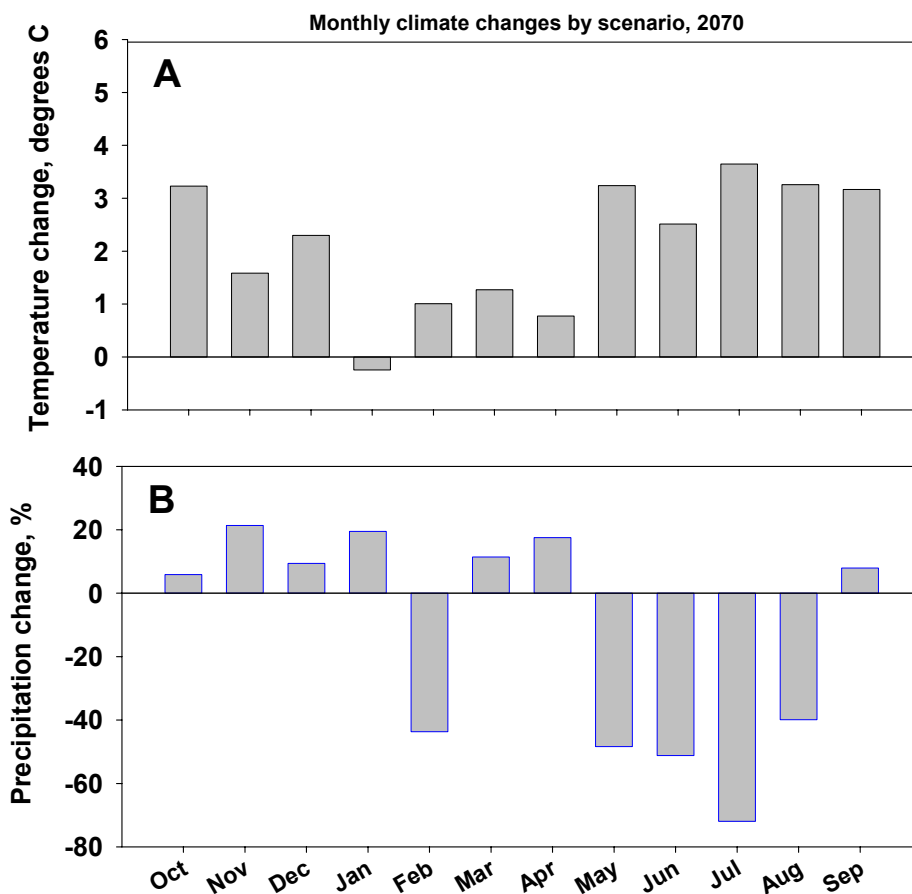


**Figure 17. Projected changes in monthly average temperature (A) and precipitation (B) from PCM-RCM in 2070.**

9. PCM-RCM projections are for 2070 (rather than 2075) because PCM-RCM analysis requires that we take an average of multiple years, centered on the time period of interest. Since PCM-RCM projections are only available to 2075, we centered our average on 2070.

PCM-RCM generally projects smaller temperature increases than MAGICC/SCENGEN and the five GCMs. Consistent with the MAGICC/SCENGEN and GCM projections, PCM-RCM projects a decrease in annual precipitation, even though precipitation may increase in some months.

### 2.6.3 SDSM

The projections of temperature and precipitation changes using statistical downscaling of the HadCM3 are shown in Table 5. The results are downscaled to the mid-mountain station at the Park City ski area, which is located at 2,813 m (9,230 ft). These temperature increases are also generally smaller than those projected by MAGICC/SCENGEN and the GCMs, but the direction and degree of precipitation change is similar.

**Table 5. Estimated changes in temperature and precipitation using statistical downscaling from HadCM3 to the mid-mountain station at Park City ski area, 2,813 m (9,230 ft)**

Year	Scenario	Temperature increase (°C)	Precipitation change (%)
2030	B2 – Moderate	1.45	-12
	A2 – High	1.05	-2
2075	B2 – Moderate	2.72	-16.5
	A2 – High	3.63	-13.5
2100	B2 – Moderate	3.26	-20
	A2 – High	4.81	-23

## 2.7 Summary

All of the emissions scenarios project a substantial increase in temperature for the Park City area over the next 100 years. Different assumptions about future emissions result in a range in average annual increase in temperature for Park City of about 1.5°C by 2100 for the SDSM projections to about 4°C by 2100 for the MAGICC/SCENGEN and GCM projections.

On average, the models project a decrease in precipitation regardless of the emissions scenario and modeling approach. One of the five GCMs projects a small increase in precipitation. Given the variability in the results, we cannot be certain about the direction or magnitude of change in precipitation.

## **3. Park City Mountain Snowpack Modeling**

### **3.1 Introduction**

We parameterized and ran a snowpack model to evaluate how snow at the Park City ski area could be affected under the climate scenarios described in Section 2. Our objectives were to estimate the length of the ski season, the timing of snowpack buildup and melt, and the snow depth and coverage at specific times and elevations.

### **3.2 Snowmelt Runoff Model**

We used the SRM to examine snowpack characteristics in the Park City ski area (Martinec, 1975; Martinec et al., 1994; <http://hydrolab.arsusda.gov/cgi-bin/srmhome>). The SRM is designed to assess snow coverage and snowmelt runoff patterns. It is based on the concept that changes in air temperature provide an index of snowmelt. The SRM calculates the maximum snow in storage on a defined winter end date. Beyond the winter end date, the SRM will model the melting process and the subsequent depletion of snow-covered area.

To model the rate and spatial distribution of snowpack buildup during the fall and early winter months, we developed an additional module for use with the SRM. Since snowpack buildup is dictated by temperature and precipitation, we used changes in temperature to determine the change in timing at which snow begins to accumulate. We scaled the rates of change in snow-covered area by changes in precipitation.

The spatial extent of this evaluation was the current (2006) Park City ski area property boundary area (17.5 km<sup>2</sup>). The property boundary encompasses a vertical relief of approximately 1,067 m (3,500 ft), from the base area at 2,100 m (6,890 ft) to the highest elevation at 3,170 m (10,400 ft). We created four elevation zones in the model to generate refined estimates of snowpack coverage. The four elevation zones each averaged 265 m (872 ft) (Figure 18).

The SRM requires current climate data and an estimate of snow-covered area. These are described in the following sections.

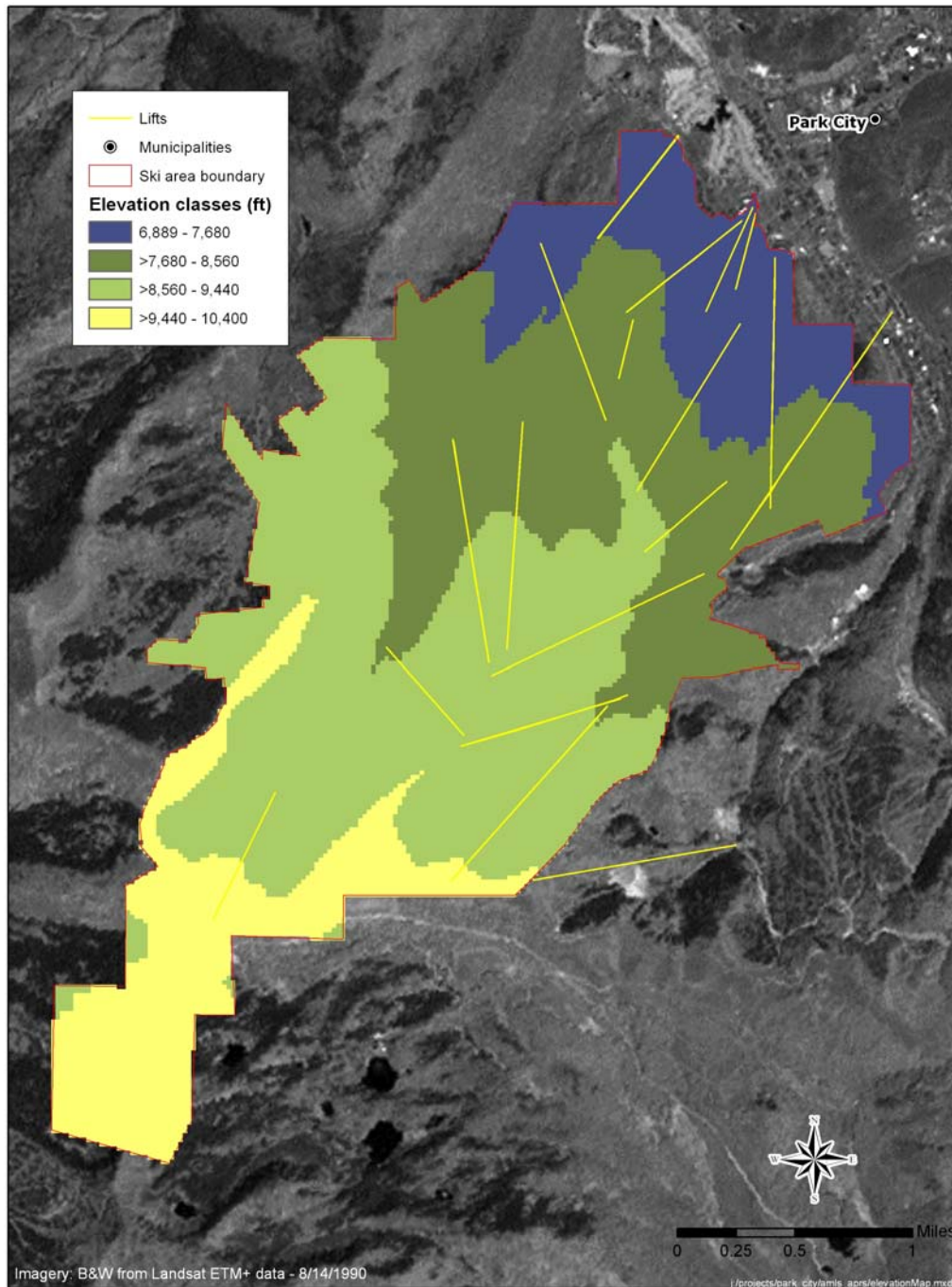


**Figure 18. Spatial extent of the SRM evaluation.** Colors identify the four elevation zones used in the model to refine estimates of snowpack from the base area to the top of the Park City ski area.

### 3.2.1 Current climate data

We identified two sources of meteorological data for the Park City ski area that were suitable for use in the SRM. The SRM requires full-year temperature and precipitation datasets. Full-year datasets were available from the weather station at the golf course in the town of Park City [elevation 2,080 m (6,824 ft)], and from the Thaynes Canyon USGS SNOTEL site located near the mid-mountain station in the ski area [elevation 2,813 m (9,230 ft)]. The golf course station is within 23 m (76 ft) of the base area elevation and is approximately a quarter mile away. We used data from the golf course to estimate conditions at the bottom of Park City Mountain. We used data from Thaynes Canyon to represent conditions from the mid to upper parts of Park City Mountain. We compared cumulative winter snowfall recorded at the Thaynes Canyon SNOTEL station and the adjacent ski area weather station (Summit station) and found that the totals matched very well (Figure 19). This allowed us to use Thaynes Canyon as a direct measure of precipitation at the Summit station for the whole year.

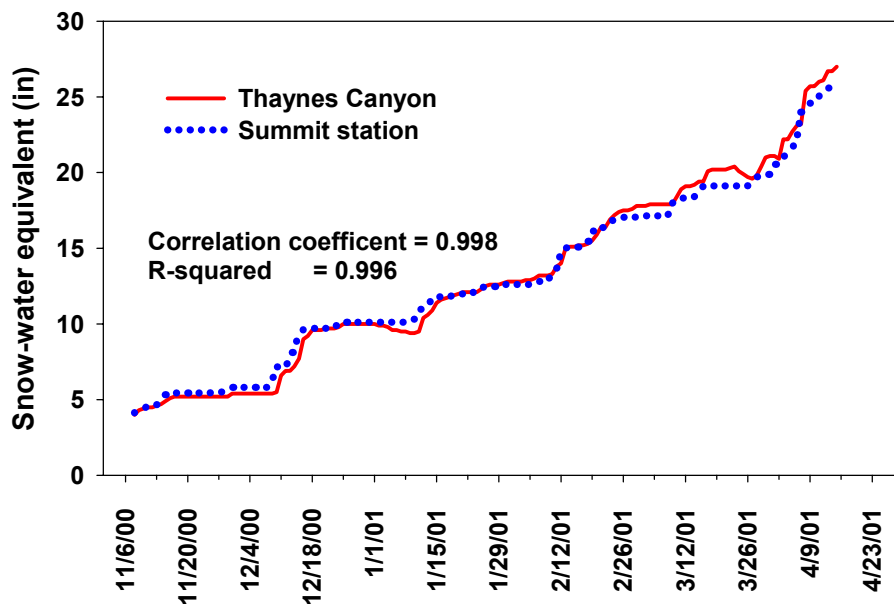


**Figure 19. Comparison of cumulative SWE between Thaynes Canyon and the mid-mountain Summit station of Park City Mountain.**

To describe temperatures at elevations between the golf course and Thaynes Canyon and above Thaynes Canyon, we estimated the rate of change in temperature with elevation, based on differences in concurrent temperatures at the two weather stations. The resulting average, which is called a lapse rate, is  $0.40^{\circ}\text{C}/100\text{ m}$ . For each 100 m increase in elevation, we expect temperature to decrease  $0.4^{\circ}\text{C}$  on average.

### 3.2.2 Snow-covered area

The SRM requires daily estimates of snow-covered area. We estimated snow-covered area using high resolution Landsat images. Since high-resolution images are expensive, we selected 2000-2001 as the year that is reasonably representative of the historical average snow-covered area. Figure 20 shows that precipitation and snow water equivalent (SWE) at Thaynes Canyon from the October 2000 through September 2001 season were similar to average precipitation and SWE from 1971 to 2000. Park City Mountain managers and snow safety directors agreed that the 2000-2001 season snowpack was representative of average conditions.

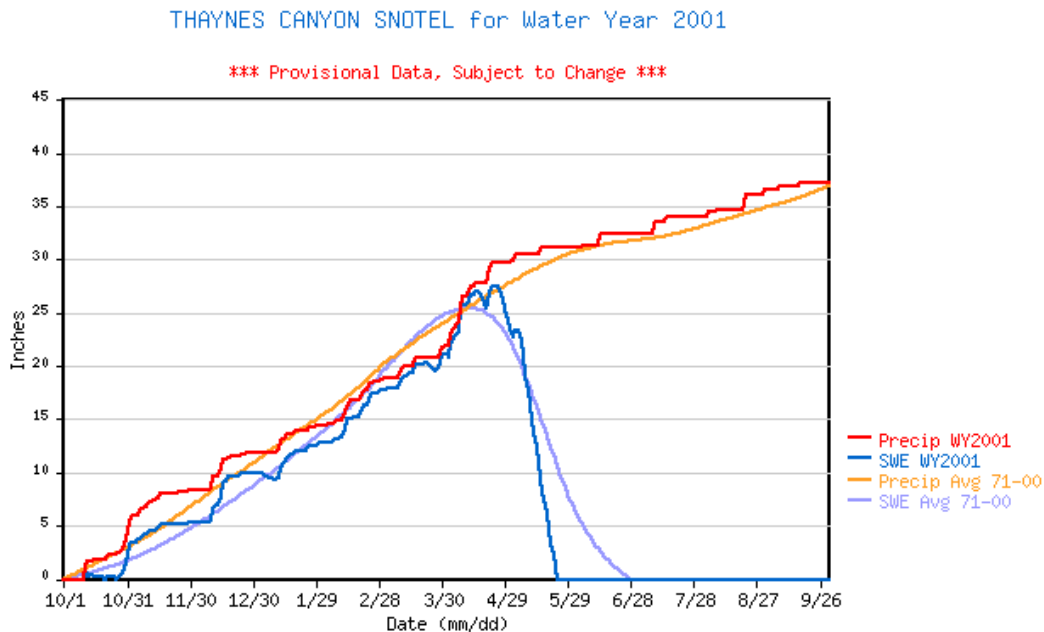


**Figure 20. SWE measured at the Thaynes Canyon USGS SNOTEL station on Park City Mountain.** The historical average is taken from 1971 to 2000. The 2000-2001 season is representative of the historical average.

Source: NRCS, 2006.

We used six Landsat (ETM+) scenes from 2000 and 2001 (October 19, December 30, January 31, March 4, April 5, and May 7) to estimate snow-covered area for the ski season. The snow-covered area for each date was combined with digital topography to derive estimates of snow-covered area by elevation band. To estimate snow-covered area on all other days, we interpolated linearly between the six scene dates (Figure 21). In Appendix D, we describe the snow cover analysis in more detail.

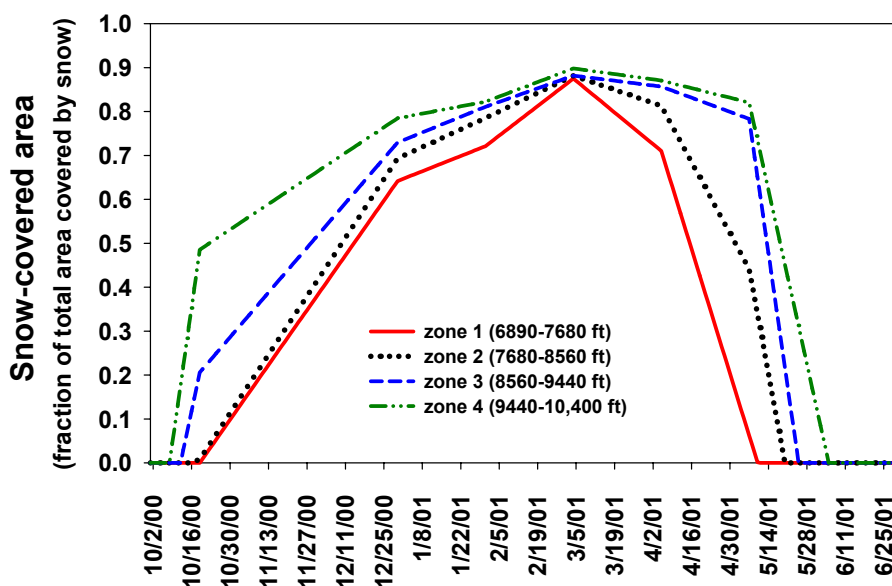


**Figure 21. Daily time series of snow-covered area by elevation zone for the 2000-2001 ski season.**

### 3.3 SRM Runs

We ran the SRM to simulate melt patterns for the 2001 water year to verify that it can accurately represent snowmelt conditions in the Park City area.<sup>10</sup> We used runoff parameters developed for similar mountainous regions of Aspen and Del Norte, Colorado. The parameters only affect projections of runoff volume, and not projections of snow-covered area depletion due to melt. Snow-covered area depletion due to melt is driven by climate variables and the snow density

10. A quantitative calibration would have required daily natural stream flow in each of the four watersheds that the ski area property spans, and many more satellite images for snow-covered area classification. Such a calibration was beyond the scope of this project.

derived degree-day factor. A degree-day is the number of days multiplied by temperature, and the degree-day factor converts degree-days to melt. A degree-day over freezing temperature produces melt, and one below freezing does not. We determined that the SRM modeled historical conditions reasonably well.

We modeled future climate change scenarios by scaling observed temperature and precipitation records by the projected monthly changes from the climate models (Section 2). The SRM generated estimated snow-covered area depletion curves from the winter end date (defined as March 1) to the end of the water year (September 30).

We applied the estimated changes in temperature from the climate models to observed historical records from the Thaynes Canyon SNOTEL station, 1988-present to estimate the change in timing and rate of snowpack buildup. For example, if the historical record suggested that a temperature increase of a given amount delays the start of snow accumulation by five days, then we applied a five-day delay to the snowpack accumulation observed in 2001. Snow-covered area rates of change were then scaled by the predicted monthly changes in precipitation.

By plotting snow-covered area and measured snow depth at the base area in 2000-2001, we developed a simple linear relationship between snow depth and snow-covered area [Figure 22, snow-covered area = (0.0257 H snow depth) + 0.0974]. Actual measured snow depth data were available from the Jupiter station at the top of Park City Mountain, the Summit mid-mountain station, and at the golf course, near the base area elevation (Figure 23). These locations lie in elevation zones 4, 3, and 1, respectively. To generate a snow depth time series for the mean of each elevation zone, we interpolated linearly between the three measured datasets (Figure 24). Since the relationship between the three measured datasets varied with date, a separate linear interpolation was conducted for each week throughout the 2000-2001 winter. We used this information to estimate future snow depths given the modeled snow-covered area. Snow depths at the golf course are not enhanced by snowmaking, and are therefore likely to underestimate observed depths at the base area. Our approach projects natural snowpack characteristics only at the base area. We did not evaluate effects of augmentation with man-made snow.

### **3.4 SRM Modeling Results**

In the following sections, we describe effects of the climate change projections on the start date of snowpack buildup, the start date of snow melt, snow-covered area, and snow depth in 2030, 2075, and 2100.

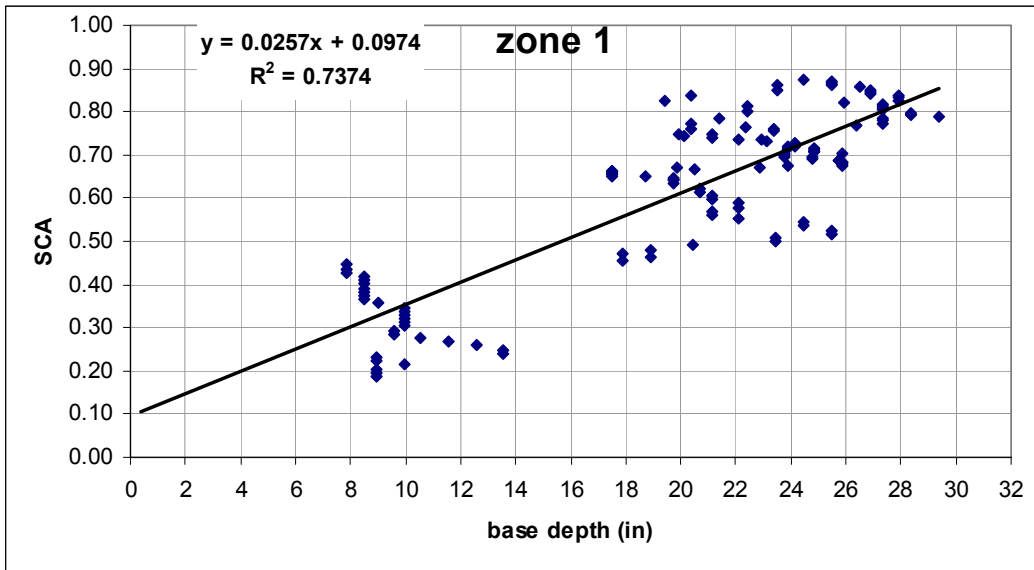


Figure 22. Example of snow-covered area vs. snow depth relationship from the base area of Park City ski area for the 2000-2001 season for zone 1 (elevation 6,889 to 7,680 ft).

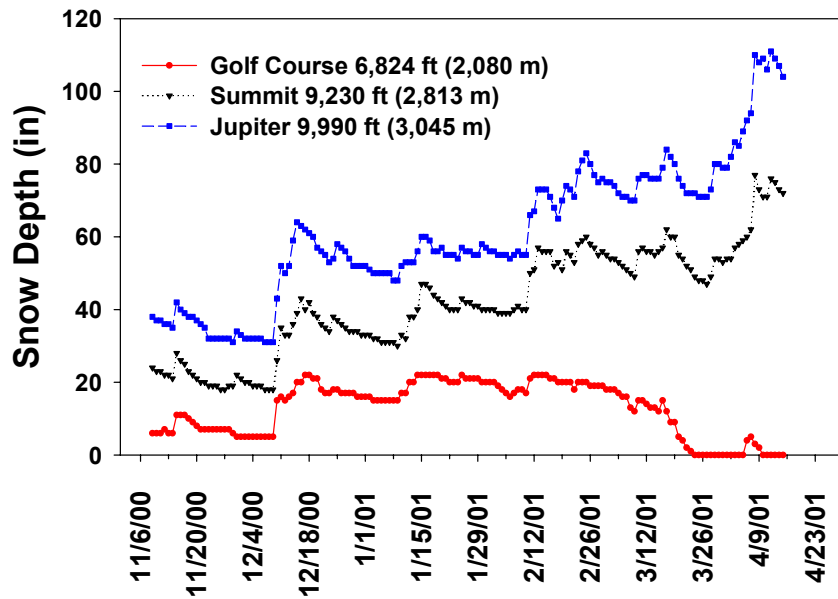
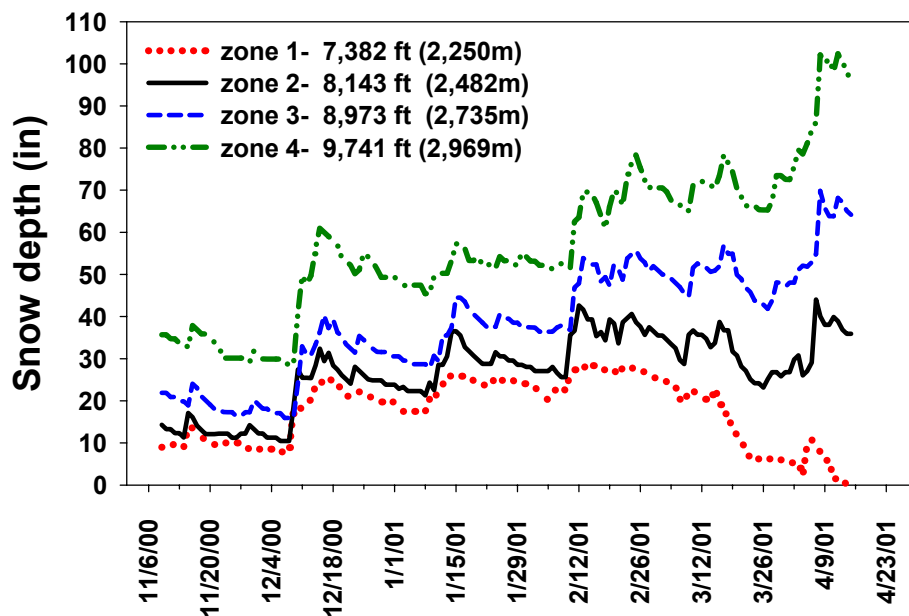


Figure 23. Measured snow depths at the golf course, mid (Summit), and top (Jupiter) of Park City Mountain.



**Figure 24. Interpolated snow depths for elevations representing each defined elevation zone in the SRM model.**

### 3.4.1 2030

The start of snowpack buildup is defined as the date when precipitation falls as snow rather than as rain and remains as snow on the ground. Historically, the start of snowpack buildup at the Park City ski area was October 30. The start of snowpack buildup at the base area of the Park City ski area is projected to begin a few days later in climate scenarios for 2030. Projected temperatures will still allow some snowpack buildup to occur before Thanksgiving, and approximately three weeks of conditions suitable for snowmaking. Snow melt at the base area is projected to begin one week to 10 days earlier than the historical melt initiation date of March 18 under the A1B scenario, and only one day earlier under the A2 and B2 scenarios using SDSM. The projected snow-covered area at Park City's base area for 2030 is shown in Figure 25. Snow depth in the early part of the snow accumulation season (November through December) is projected to be near historically observed depths. By late February, snow depth is projected to be below historically observed maximum depths (Figure 26). For all scenarios in 2030, melt begins earlier than historically. The result is slightly reduced snow depth by spring break due to earlier melt initiation. If the early snowmelt date causes less than a 50% of snowpack reduction by March 25, then skiable snow should remain at the base area throughout the spring break season in 2030.

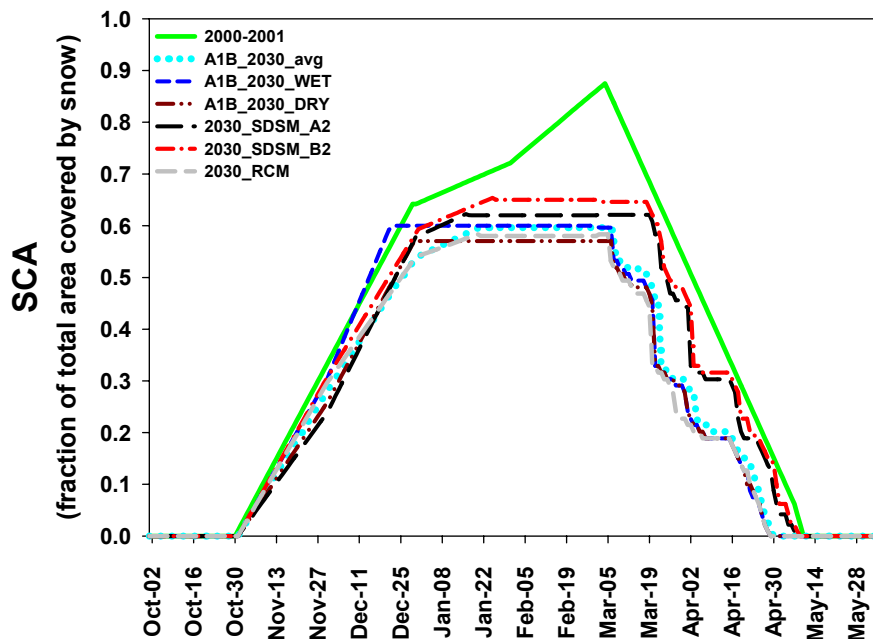


**Figure 25. Modeled snow-covered area time series at Park City's base area for future climate scenarios in 2030. 2000-2001 represents historically observed depths.**

The impact of climate change at the top of mountain will be less pronounced (Figure 27). The start of snowpack buildup at the top of the Park City ski area will begin two to six days later than the historical start date of October 22. The A1B\_WET (CSIRO) and SDSM scenarios eventually come very close to the historical maximum snow coverage and depth because of minimal (0.6-1.5°C) winter warming and slightly increased winter precipitation. In the A1B\_avg, A1B\_DRY (ECHAM3), and PCM-RCM scenarios, winter precipitation will either remain near current levels or decrease, and winter temperature increases are larger (1.4-1.8°C) than A1B\_WET and SDSM scenarios. This causes predicted maximum snow depths to be slightly below historical maximums (Figure 28). Although melt initiation is projected to occur two to three weeks earlier than the historical melt initiation date of April 14 for the A1B scenarios, the melt effects will be only minimally apparent by the end of March.

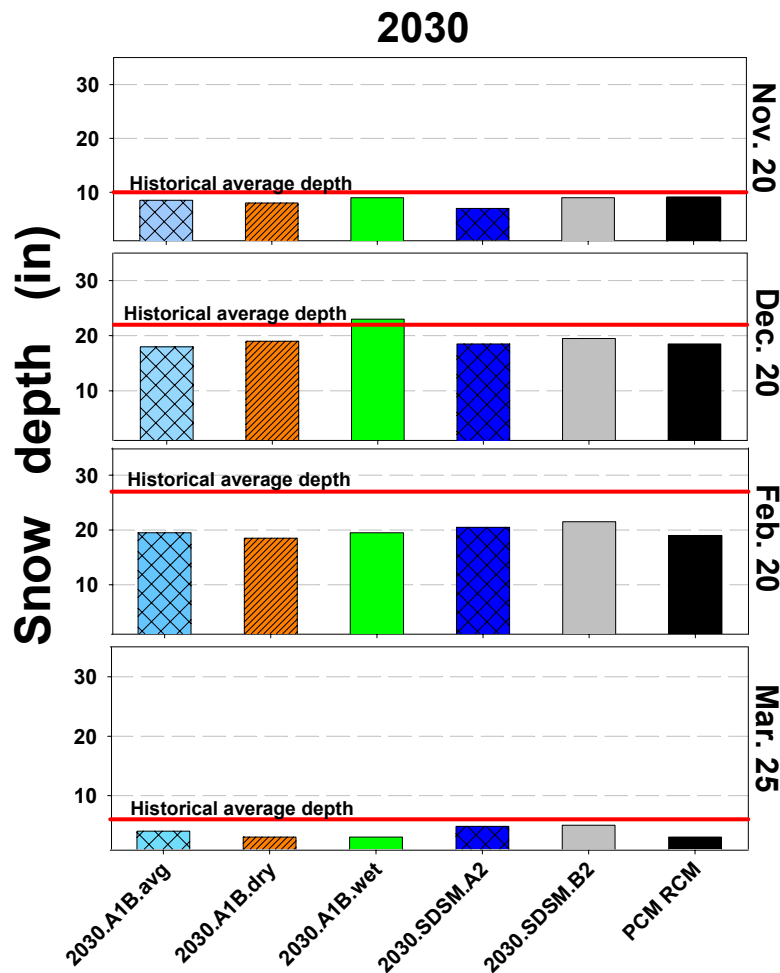
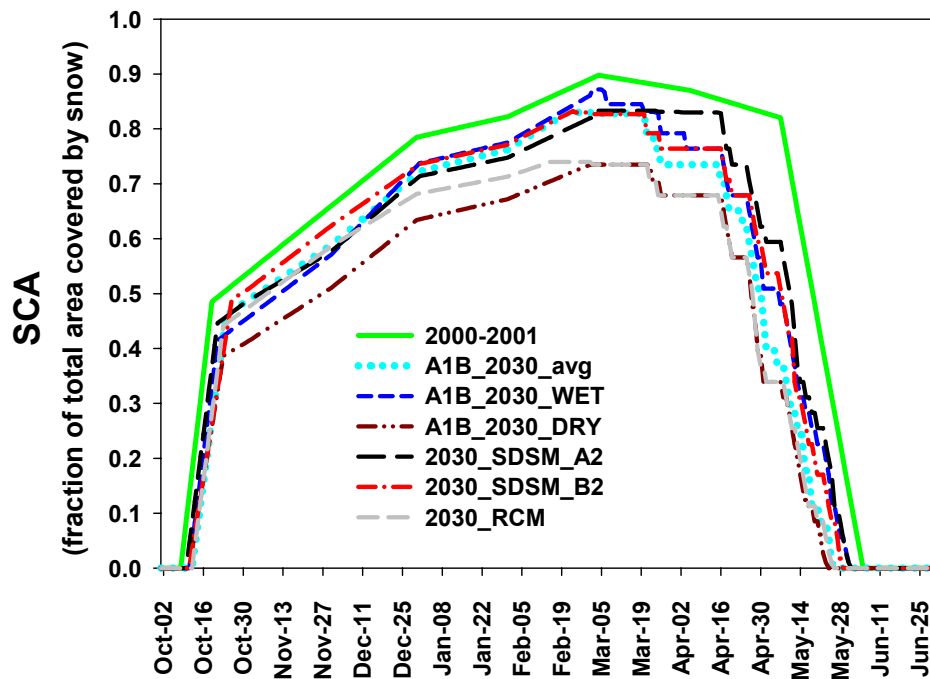


Figure 26. Estimated snow depths at Park City’s base area for 2030.

### 3.4.2 2075

By 2075, climate change is projected to have a substantial impact on snow coverage and snow depth at Park City’s base area. Snowpack buildup will be delayed by 3.5 weeks for the MAGICC/SCENGEN and GCMs projections with A1B and B1 emission scenarios, and by almost two months for the A1FI scenario. The PCM-RCM and SDSM scenarios project snow accumulation delays of 20 to 24 days. The projected snow-covered areas at Park City’s base area for 2075 are shown in Figure 29. The RCM results are for 2070.



**Figure 27. Modeled snow-covered area time series at the top of Park City ski area for future climate scenarios in 2030.**

Melt at the base area will occur periodically throughout the winter, beginning as early as late December to early January for the A1B, B1, and A1FI scenarios, and in early March for the RCM and SDSM scenarios. The resulting impacts on estimated snow depths are shown in Figure 30. For all scenarios, there will be either very little or no snow at the base area by Thanksgiving, and mid-winter snow depths will be 28% to 100% less than historically observed values. By the spring break season, snow depths are predicted to be almost zero for all scenarios due to an earlier onset of melt. Under the high emission A1FI scenario, there is unlikely to be a persistent seasonal snowpack at the base area, and the snow line will move up to approximately 2,900 m (9,500 ft).

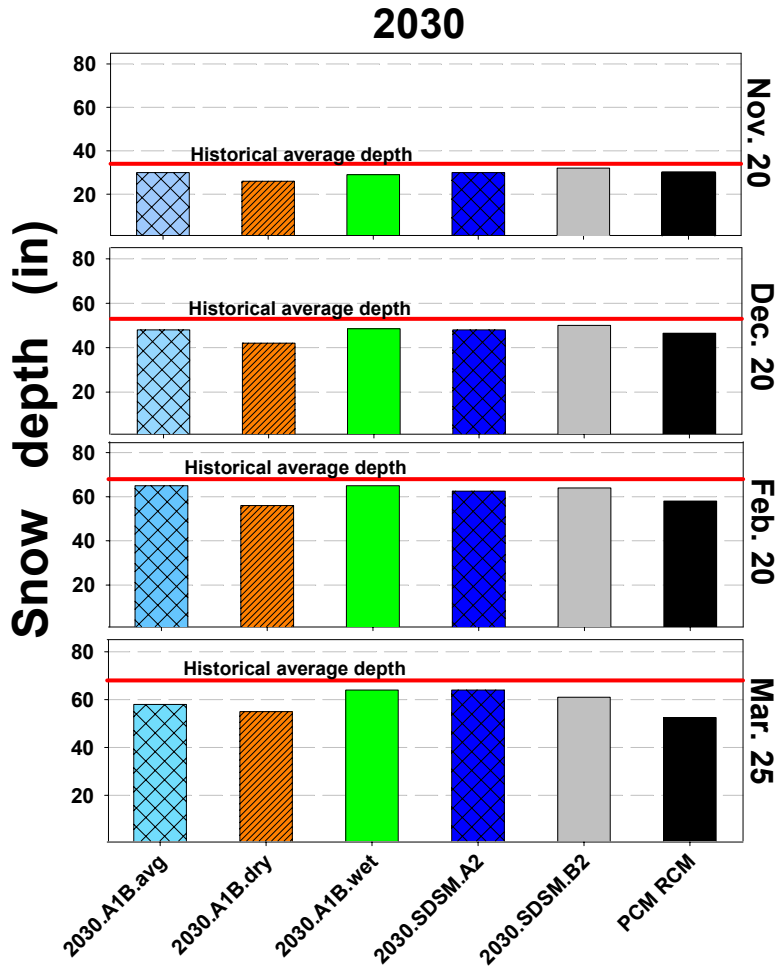
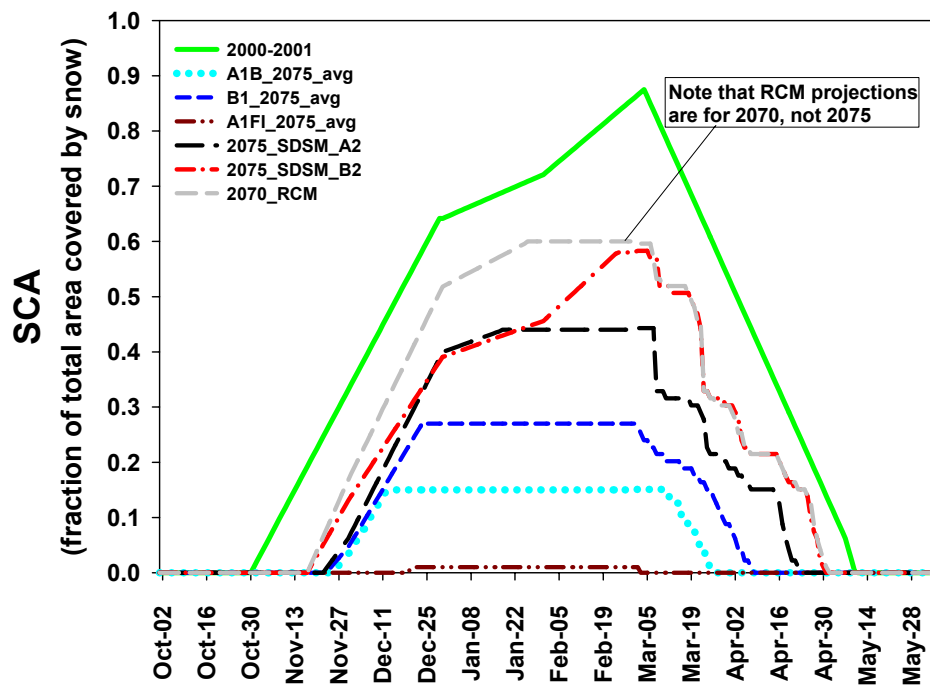


Figure 28. Snow depths at the top of Park City ski area for 2030.



**Figure 29. Modeled snow-covered area at Park City's base area for future climate scenarios in 2075.**

The impact at the top of Park City Mountain will not be as dramatic as that projected for the base area, although changes in snow coverage and depths are projected to be substantial. Initiation of snow accumulation will be delayed by a week to 10 days for the B1 and A1B scenarios, and by 3.5 weeks for the A1FI scenario. The PCM-RCM and SDSM scenarios project delays of about five to 10 days. Figure 31 shows estimated snow-covered area for all scenarios at the top of Park City Mountain in 2075. Melt initiation at the top of the ski area will occur four to five weeks earlier for the A1B, B1, and A1FI scenarios, and one to three weeks earlier for the RCM and SDSM scenarios. The estimated snow depths are shown in Figure 32. The delay in snow accumulation will result in reduced early to mid-winter snow depths. Spring snow depths will be further impacted by earlier melt initiation, resulting in more pronounced snow depth reductions, and no snow in the A1FI scenario. In 2075, the top of Park City is projected to have a persistent (albeit reduced) snowpack for at least some portion of the early winter to spring operating season.

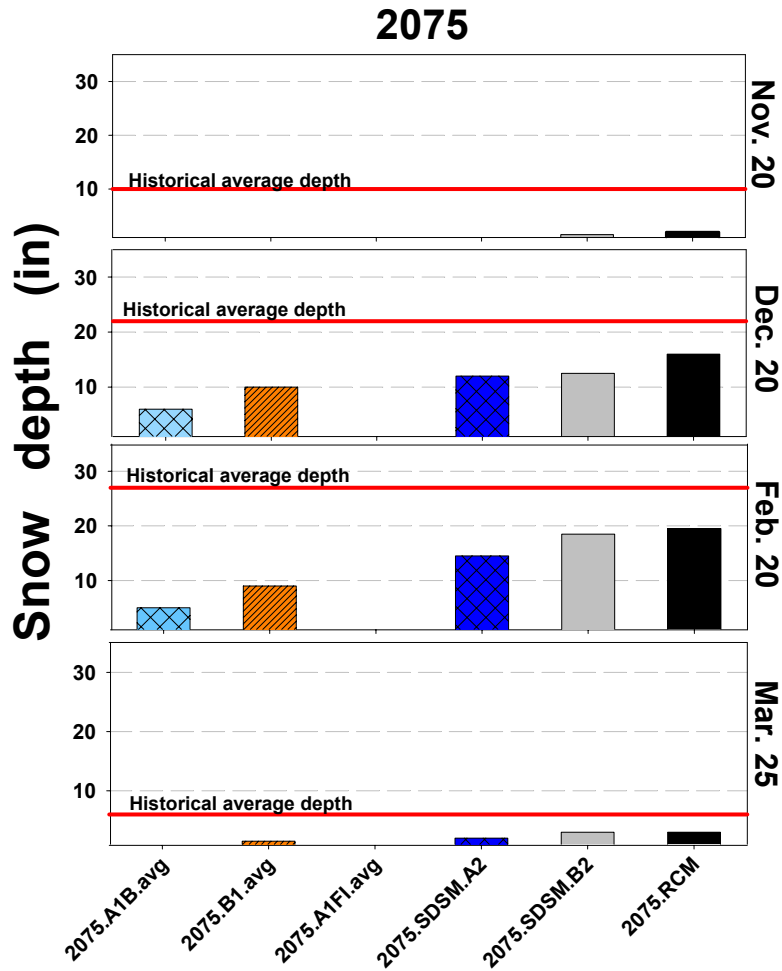


Figure 30. Base area snow depths at Park City for 2075.

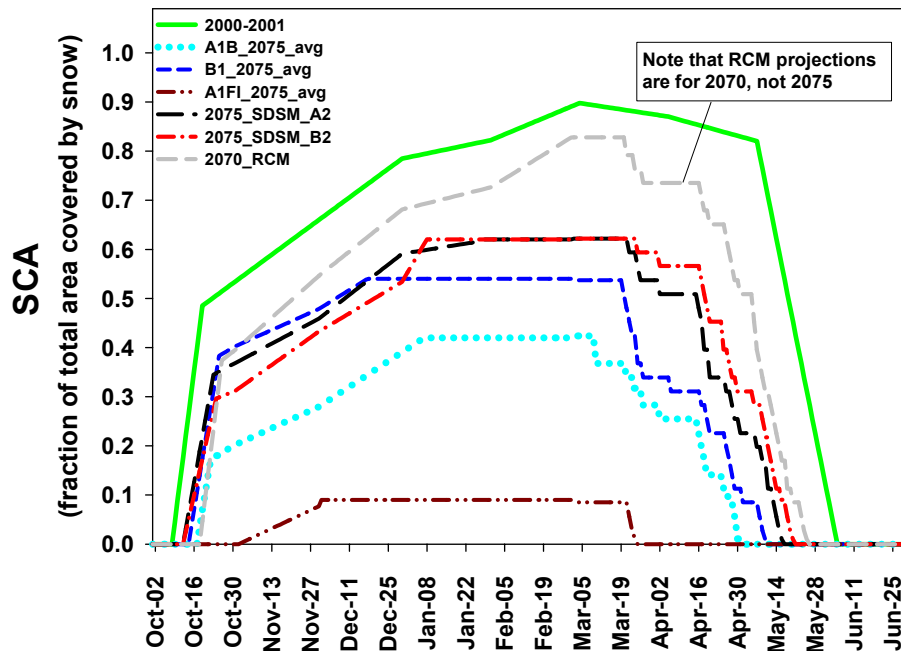
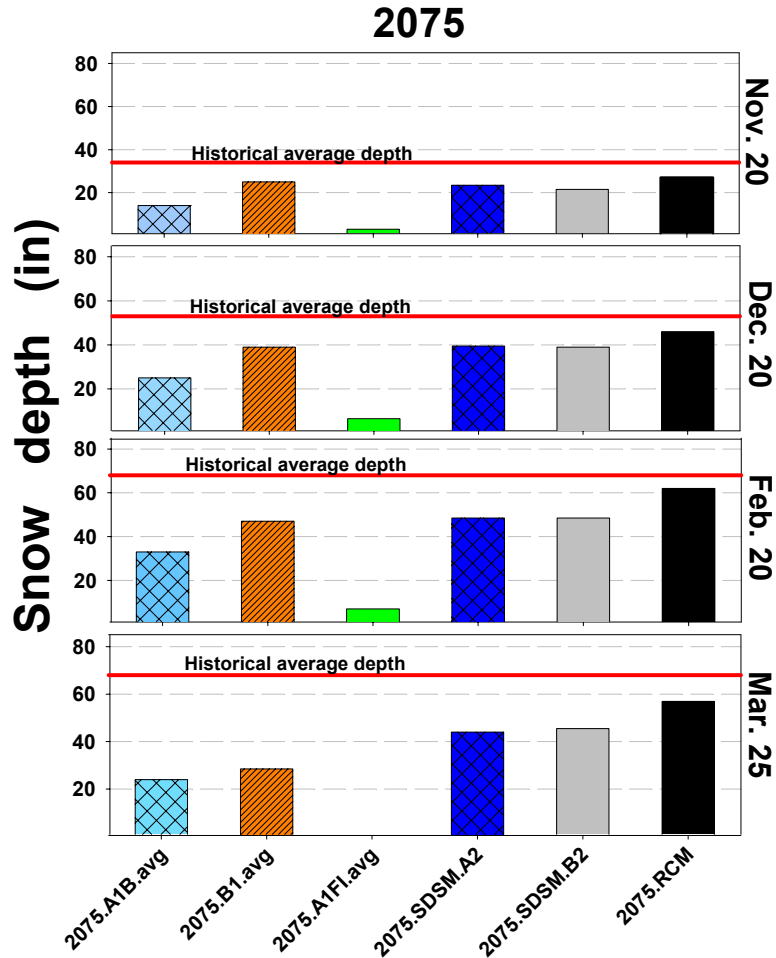


Figure 31. Modeled snow-covered area time series at the top of Park City ski area for future climate scenarios in 2075.

### 3.4.3 2100

Under the A1B and A1FI emission scenarios, by 2100 the base area of Park City Mountain will not have a skiable snowpack. Snowfall for these scenarios is projected to be infrequent or to not occur at all throughout the winter. The winter will be punctuated by frequent and sustained periods of melt.

The snow line will move up to approximately 2,900 m (9,500 ft) for the A1B scenario, and to approximately 3,100 m (10,200 ft) for the A1FI scenario. Under the B1 (low emissions) scenario using the GCM average and under the SDSM scenarios, a snowpack will eventually develop at the base area by mid-winter. Under these scenarios, snow coverage and depths at the base area will be substantially reduced, but not completely obliterated.



**Figure 32. Snow depths at the top of Park City Mountain in 2075.**

The start of snowpack buildup at the base area of Park City Mountain in 2100 is projected to begin from one to two months later than the historical start date of October 30. For the A1FI scenario, snowpack buildup will not occur at all, and all winter precipitation will come as rain. Snow melt at the base area will occur throughout the winter for the A1B and B1 scenarios; six weeks earlier than the historical melt initiation date of March 18 for the SDSM A2 scenario; and 10 days earlier for the SDSM B2 scenario. Figure 33 shows estimated snow-covered area at the base area of Park City for 2100.

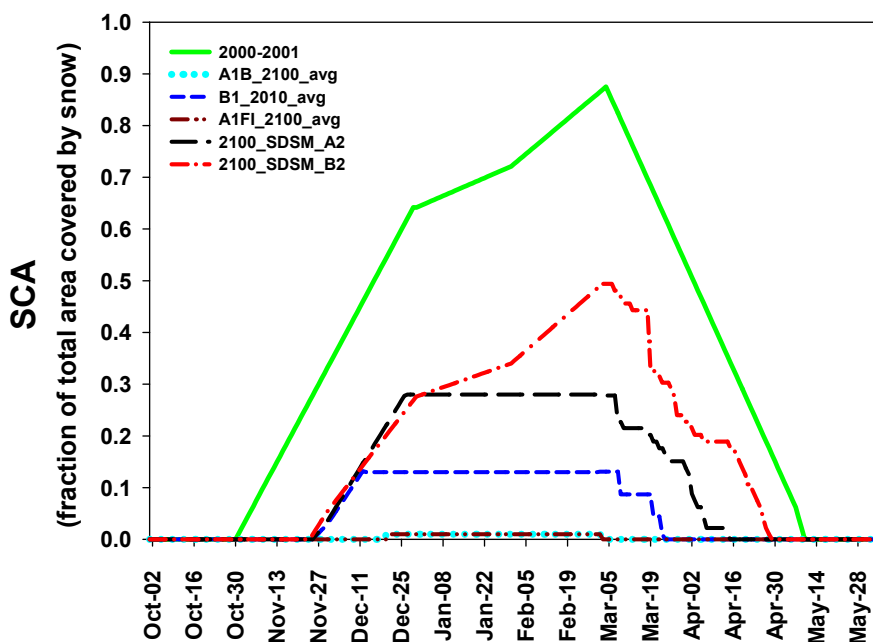


**Figure 33. Modeled snow-covered area time series Park City's base area for future climate scenarios in 2100.**

Skiable snow may only exist at the base area under the B1-GCM model average and SDSM scenarios. Figure 34 illustrates how significantly base area snow depths may be affected by 2100. Snow depth maximums for the A1B and A1FI scenarios occur by February 20, and only reach 19% to 54% of the historical maximum. By 2100, snow depths during March are substantially reduced for all scenarios to the point where skiing may no longer be possible during the busy spring break season.

The conditions at the top of the mountain [2,877-3,170 m (9,300-10,400 ft)] show less sensitivity to the A1B, B1, and SDSM scenarios than the base area, but substantial sensitivity to the A1FI scenario. The cooler temperatures at this higher elevation insulate the snowpack from potential warming enough to maintain a seasonal snowpack in all but the A1FI high emissions scenario (Figure 35). The snow deficit caused by October precipitation coming as rain is never regained, as indicated by maximum snow-covered area values below the historical average values. Melt initiation occurs four to five weeks earlier under the A1B, B1, and SDSM A2 scenarios, and 10 days earlier for the SDSM B2 scenario. Melt conditions occur throughout the winter for the A1FI scenario. Skiable snow would probably exist at the top of the mountain under the A1B, B1, and SDSM scenarios, although snow depths would be significantly reduced (Figure 36). Snow will not be present under the A1FI scenario.

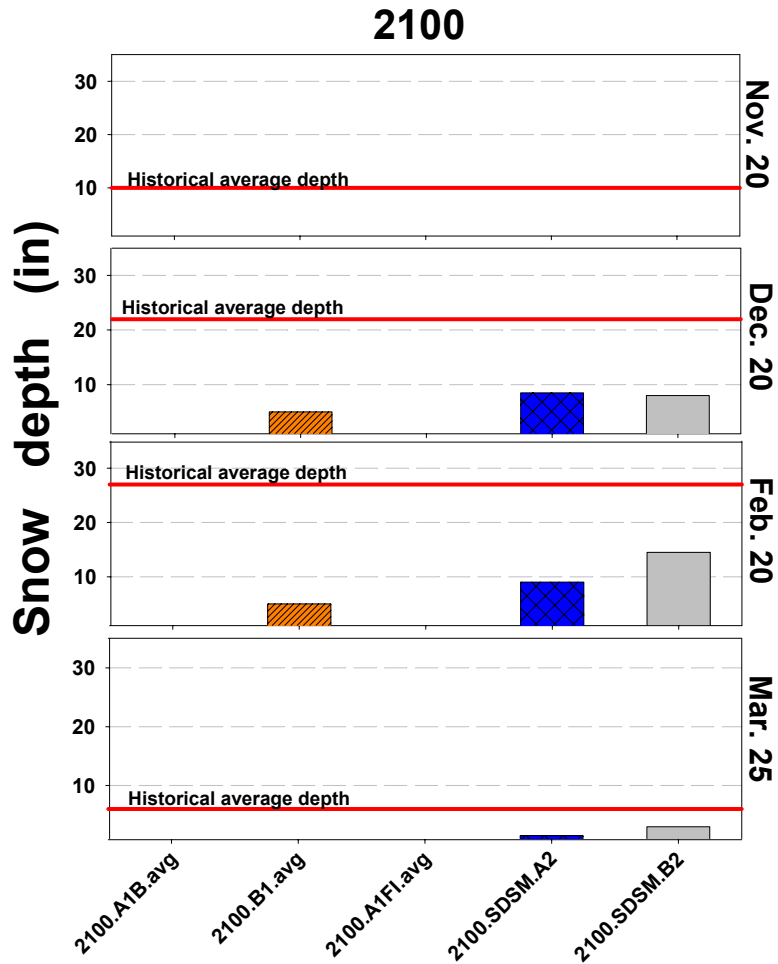


Figure 34. Base area snow depths at Park City for 2100.

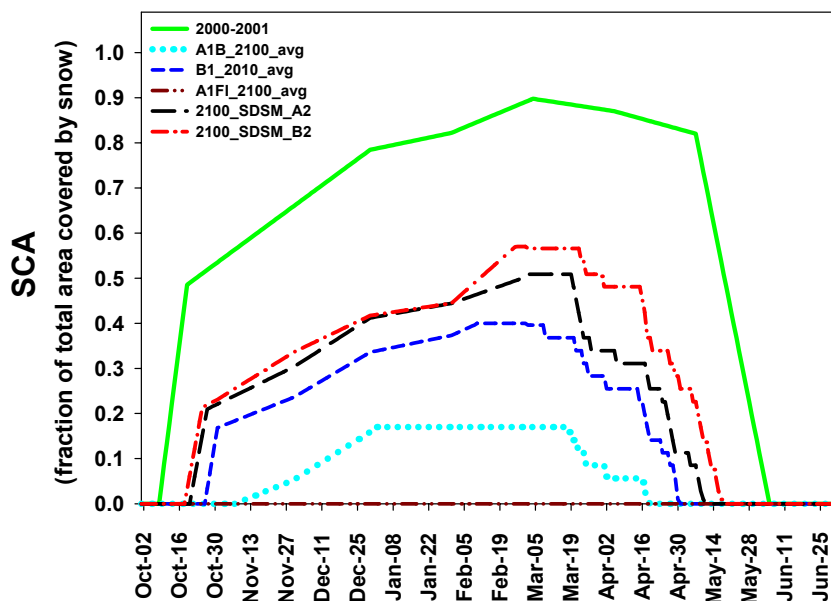


Figure 35. Modeled snow-covered area for the top of Park City Mountain in 2100.

### 3.5 Snowpack Summary

We estimate that the projected rising temperatures will delay the date that snow starts to accumulate at the Park City base area by a few days by 2030, three to seven weeks by 2075, and from four weeks to no accumulation at all by 2100. In most scenarios, the delayed accumulation causes the maximum snow depths to fall short of the historical maximum. Predicted snow depth in 2030 during spring break is about 17% to 50% lower at the base area than in 2000-2001, with a small decrease in depth near the top of the mountain. The onset of melt, and the spring avalanche cycle, is predicted to start earlier by one to three weeks in all model runs. All model runs show skiable snow for all elevations and dates on Park City in 2030, but not in 2075.

Thanksgiving and spring break snow depths are projected to be at or near zero for all scenarios in 2075 at the base area. For the A1FI scenario, persistent seasonal snowpack at the base area is unlikely, and the snow line will move up to approximately 2,900 m (9,500 ft). The top of the ski area will maintain skiable snow throughout the ski season in all but the A1FI scenario, although snow depths will be reduced by 15% to 65% compared to historical depths.

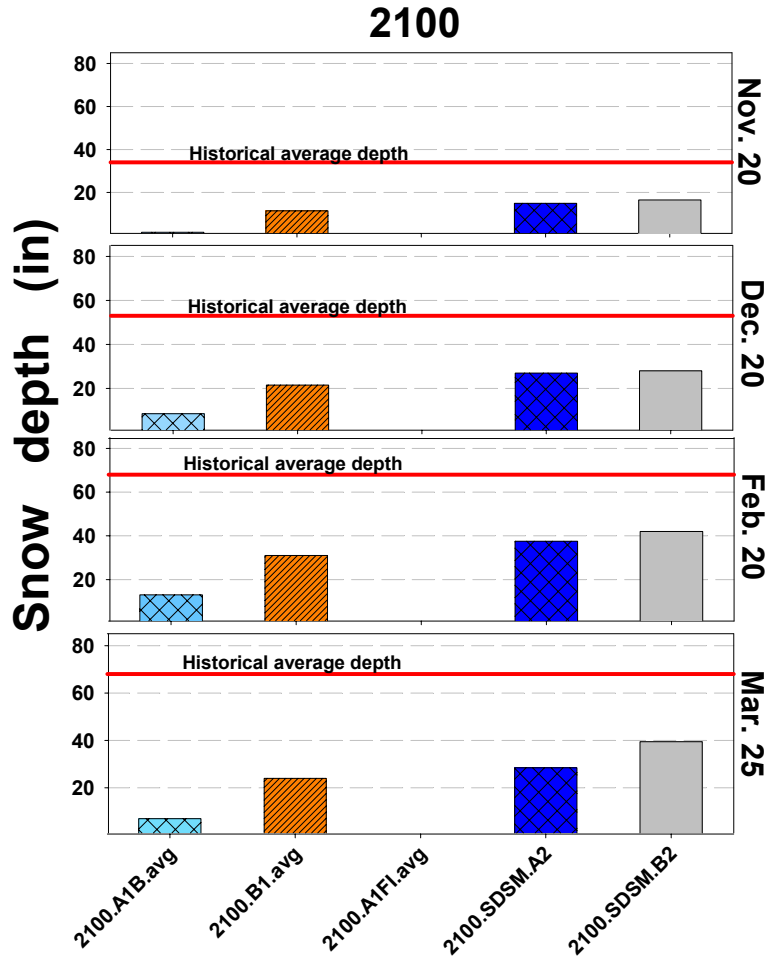


Figure 36. Snow depths at the top of Park City Mountain in 2100.

By 2100, only the B1 and SDSM scenarios project skiable snow at the base area, and only during December through February. Results for the A1B scenario for 2100 indicate that a persistent snowpack will exist only for the upper quarter of the mountain. For the A1FI scenario, persistent snow coverage does not exist anywhere on the mountain.

## 4. Uncertainty

As noted in Section 2, there is uncertainty about the magnitude of warming in Park City. In addition, whether precipitation will increase or decrease is uncertain. The change in precipitation as a result of GHG emissions is more uncertain than the future temperature change. In addition to uncertainty about how the climate in Park City will respond to GHG emissions, and exactly what those emission levels will be in the future, there is uncertainty inherent in the snow modeling.

Snow coverage and depths were determined based on changes from observed coverage and depth for a single representative ski season in 2000-2001. However, individual years may exhibit variability with greater or smaller snow coverage and depth values than those observed in 2000-2001. This year-to-year variability is not accounted for in the snowpack modeling. It should be noted that snow depths at the golf course are not enhanced by snowmaking, and are therefore likely to underestimate observed depths at the base area. Our approach projects natural snowpack characteristics only at the base area. We did not evaluate effects of augmentation with man-made snow.

## 5. Conclusions

GHG concentrations are expected to continue to rise and climate to change. In Park City, temperature will probably increase substantially over the coming century. The amount of warming depends on future GHG emissions and how they affect climate in the Rockies. Different assumptions about emissions result in projected warming ranging from 3.3° to 8.4°C (5.9° to 15.1°F) by 2100 over temperatures in Park City in the 1990s. By the century's end, Park City's climate may resemble the current climate of Salt Lake City. Warming is projected to be more pronounced during summer months than winter months.

On average, the models project a decrease in annual precipitation, a small increase in winter precipitation, and a substantial decrease in summer precipitation, regardless of the emissions scenario or modeling approach. However, because of the variability between models, we cannot be sure whether precipitation over the central Rockies will decrease or increase over the 21st century.

Using the climate change scenarios and the SRM, we estimate that the date when snow starts to accumulate at the Park City base area will be delayed a few days by 2030, three to seven weeks by 2075, and from four weeks to no accumulation at all by 2100. In 2030, all model runs show skiable snow for all elevations and dates throughout the ski season, but not by 2075.

Thanksgiving and spring break snow depths at the base area are projected to be at or near zero for all scenarios in 2075, and a persistent snowpack will exist only above 2,900 m (9,500 ft) under the high emission scenario. The top of the ski area is projected to maintain skiable snow throughout the ski season in 2075 in all but the high emission scenario, but snow depths are reduced by 15% to 65%, compared to historical observations. By 2100, only the low GHG emissions and low climate change scenarios maintain skiable snow, and only from December through February at the base area. Results for a middle emissions scenario for 2100 indicate that a persistent snowpack will exist only for the upper quarter of the mountain. Under the very high emissions scenario, there will be no persistent snow cover.

Snowpack begins to be substantially impacted when winter temperatures warm more than approximately 2° to 3°C (4° to 5°F). Climate model results suggest that winter warming in the central Rocky Mountains is approximately one third greater than the GMT. This implies Park City might experience a 2° to 3°C warming when the GMT warming is only 1.5° to 2.3°C (3° to 4°F). Such an increase in temperature could be realized by mid-century.

It is unlikely that early season reductions in snowpack can be offset with snowmaking by 2075, since temperatures will not become cold enough until late November to early December. Additional snowmaking later into the winter months, however, could bolster the snowpack enough to maintain skiable snow later into the spring break season. The economic implications of additional snowmaking, and other potential adaptation strategies, such as downloading skiers in the spring, may need to be considered by Park City ski area owners and operators in the face of a changing climate.

The modeling results are intended to provide a range of possible and plausible future scenarios to assist ski area managers in assessing the consequences of climate change. The results should be interpreted with the realization that there is uncertainty in predicting future emissions, the effect of emissions on climate, and the effect of climate changes on snowpack characteristics.

The snow modeling provides a prediction of trends and overall average changes in snowpack characteristics as a result of future changes in climate. Snow coverage and depths were determined based on changes from observed coverage and depth for a representative ski season, but snow coverage and depth in individual seasons can vary greatly. This year-to-year variability is not accounted for in the snowpack modeling. The results should not be interpreted as an accurate prediction of precise snow depths on a particular date. The actual depth will be influenced by many factors, including natural year-to-year variability in climate, that were not accounted for in this modeling effort.

## References

- AGCI. 2006. *Climate Change and Aspen: An Assessment of Impacts and Potential Responses*. ISBN 0-9741467-3-0. Prepared for the City of Aspen by the Aspen Global Change Institute, Center of the American West, Rural Planning Institute, Stratus Consulting Inc., and Wildlife & Wetland Solutions, LLC. Aspen Global Change Institute, Aspen. July.
- Andronova, N.E. and M.E. Schlesinger. 2001. Objective estimation of the probability distribution for climate sensitivity. *Journal of Geophysical Research* 106:22,605-22,612.
- Barnett, T.P., J.C. Adam, and D.P. Lettenmaier. 2005. Potential impacts of a warming climate on water availability in snow dominated regions. *Nature* 438:303-309.
- Borys, R.D., D.H. Lowenthal, S.A. Cohn, and W.O.J. Brown. 2003. Mountaintop and radar measurements of anthropogenic aerosol effects on snow growth and snowfall rates. *Journal of Geophysical Research Letters* 30(10):1538.
- Climate Impacts Group. 2006. Hydrology and Water Resources, Key Findings. Available: <http://www.cses.washington.edu/cig/res/hwr/hwrkeyfindings.shtml>. Accessed 5/31/2006.
- Dai, A., W.M. Washington, G.A. Meehl, T.W. Bettge, and W.G. Strand. 2004. The ACPI climate change simulations. *Climatic Change* 62(1-3):29-43.
- Dozier, J. and T. Painter. 2004. Multispectral and Hyperspectral remote sensing of alpine snow properties. *Annual Review of Earth Planet Science* 32:465-94.
- Forest, C.E., P.H. Stone, A.P. Sokolov, M.R. Allen, and M.D. Webster. 2002. Quantifying uncertainties in climate system properties with the use of recent climate observations. *Science* 295:113-117.
- Galloway, R.W. 1988. The potential impact of climate changes on Australian ski fields. In *Greenhouse: Planning for Climatic Change*, G.I. Pearman (ed.). CSIRO, Melbourne, pp. 428-437.
- GLCF. 2004. Institute for Advanced Computer Studies, University of MD. Global Land Cover Facility. Available: [ftp://ftp.glcg.umiacs.umd.edu/glcg/Landsat/WRS2/p038/r032/p038r032\\_7x19990814.ETM-EarthSat-Orthorectified/](ftp://ftp.glcg.umiacs.umd.edu/glcg/Landsat/WRS2/p038/r032/p038r032_7x19990814.ETM-EarthSat-Orthorectified/). Accessed 5/30/2006.
- Hennessey, K., P. Whetton, I. Smith, J. Bathols, M. Hutchinson, and J. Sharples. 2003. *The Impact of Climate Change on Snow Conditions in Mainland Australia*. CSIRO Atmospheric Research, Aspendale, Victoria, Australia.

Houghton, J.T., Y. Ding, D.J. Griggs, M. Noguer, P.J. van der Linden, D. Xiaosu, and K. Maskell (eds.). 2001. *Climate Change 2001: The Scientific Basis*. Cambridge University Press, New York.

Kerr, R.A. 2004. Three degrees of consensus. *Science* 305:932-934.

Klein, A.G., D.K. Hall, and K. Siedel. 1998. Algorithm intercomparison for accuracy assessment of the MODIS snow – mapping algorithm. Proceedings of the 55th Annual Eastern Snow Conference, Jackson, NH, June 2-3, 1998, pp. 37-45.

König, U. 1998. *Tourism in a Warmer World: Implications of Climate Change Due to Enhanced Greenhouse Effect for the Ski Industry in the Australian Alps*. Wirtschaftsgeographie und Raumplanung, Vol. 28. University of Zurich.

Leavesley, G.H., M.D. Branson, and L.E. Hay. 1992. Using coupled atmospheric and hydrological models to investigate the effects of climate change in mountainous regions. In *Proceedings of Symposium on Managing Water Resources During Global Change, Reno, Nevada*. American Water Resources Association, pp. 691-700.

Leung, L.R. and Y. Qian. 2005. Hydrologic response to climate variability, climate change, and climate extreme in the U.S.: Climate model evaluation and projections. In *Regional Hydrological Impacts of Climatic Change – Impact Assessment and Decision Making*, Wagener, T., S. Franks, V. Gupta Hoshin, E. Bogh, L. Bastidas, C. Nobre, and C. de Oliveira Galvao (eds.). IAHS Publication 295, pp. 37-44.

Leung, L.R., Y. Qian, and X. Bian. 2003a. Hydroclimate of the western United States based on observations and regional climate simulation of 1981-2000. Part I: Seasonal statistics. *Journal of Climate* 16(12):1892-1911.

Leung, L.R., Y. Qian, X. Bian, and A. Hunt. 2003b. Hydroclimate of the western United States based on observations and regional climate simulation of 1981-2000. Part II: Mesoscale ENSO anomalies. *Journal of Climate* 16(12):1912-1928.

Leung, L.R., Y. Qian, X. Bian, W.M. Washington, J. Han, and J.O. Roads. 2004. Mid-century ensemble regional climate change scenarios for the western United States. *Climatic Change*, 62(1-3):75-113.

Martinec, J. 1975. Snowmelt-runoff model for stream flow forecasts. *Nordic Hydrology* 6(3):145-154.

- Martinec, J., A. Rango, and R. Roberts. 1994. *The Snowmelt Runoff Model (SRM) User's Manual*, M.F. Baumgartner (ed.). Geographica Bernensia, Department of Geography, University of Berne, Switzerland.
- McBoyle G.R. and G. Wall. 1992. Great lakes skiing and climate change. In *Mountain Resort Development*, A. Gill and R. Hartmann (eds.). Centre for Tourism Policy and Research, Simon Fraser University, Burnaby, pp. 70-81.
- McCabe, G.J.J. and L.E. Hay. 1995. Hydrological effects of hypothetical climate change in the East River Basin, Colorado, USA. *Hydrological Sciences Journal* 40:303-318.
- McCarthy, J., O. Canziani, N. Leary, D. Dokken, and K. White (eds.). 2001. *Climate Change 2001: Impacts, Adaptation, and Vulnerability*. Cambridge University Press, New York.
- McReynolds, W. 2006. Park City 10 ft Contour Digital Data. Stantec Consulting Inc., Salt Lake City, UT.
- Mote, P.W., A.F. Hamlett, P.W. Clark, and D.P. Lettenmaier. 2005. Declining mountain snow pack in western North America. *Bulletin of the American Meteorological Society* 86:39-49.
- Nakićenović, N. and R. Swart (eds.). 2000. *Special Report on Emissions Scenarios*. Cambridge University Press, Cambridge, UK.
- National Assessment Synthesis Team. 2000. *Climate Change Impacts on the United States: The Potential Consequences of Climate Variability and Change*. US Global Change Research Program, Washington, DC.
- Nolin, A.W. and C. Daly. Mapping “at-risk” snow in the Pacific Northwest, U.S.A. *Journal of Hydrometeorology*. Forthcoming.
- NRCS. 2006. Site Information and Reports for Thaynes Canyon. Natural Resources Conservation Service. Available: <http://www.wcc.nrcs.usda.gov/snotel/snotel.pl?sitenum=814&state=ut>. Accessed 10/18/2006.
- Rango, A. and J. Martinec. 1997. Water storage in mountain basins from satellite snow cover monitoring. *Remote Sensing and Geographic Information Systems for Design and Operation of Water Resources Systems (Proceedings of Rabat Symposium S3, April 1997)*. IAHS Publ. No. 242, pp. 83-91.
- Rango, A. and J. Martinec. 1999. Modeling snow cover and runoff response to global warming for varying hydrological years. *World Resource Review* 11(1):76-91.

Rango, A. and J. Martinec. 2000. Hydrological effects of a changed climate in humid and arid mountain regions. *World Resource Review* 12(3):493-508.

Schröter, D. 2005. Vulnerability to Changes in Ecosystem Services. CID Graduate Student and Postdoctoral Fellow. Working Paper No. 10. July. Available: [www.cid.harvard.edu/cidwp/pdf/grad\\_student/010.pdf](http://www.cid.harvard.edu/cidwp/pdf/grad_student/010.pdf). Accessed 11/2/2005.

Scott, D. and B. Jones. 2005. Climate Change & Banff National Park: Implications for Tourism and Recreation. Report prepared for the Town of Banff. University of Waterloo, Waterloo, ON.

Scott, D., G. McBoyle, and B. Mills. 2003. Climate change and the skiing industry in southern Ontario (Canada): Exploring the importance of snowmaking as a technical adaptation. *Climate Res.* 23:171-181.

Scott, D, G. McBoyle, and A. Minogue. Climate Change and Quebec's Ski Industry. *Global Environmental Change: Human Policy and Dimensions*. Manuscript No. GEC-D-05-00011R1. Submitted for publication May 17, 2006. Forthcoming.

Seidel, K., C. Ehrlter, and J. Martinec. 1998. Effects of climate change in water resources and runoff in an Alpine Basin. *Hydrological Processes* 12:1659-1669.

Tegart, W.J. McG., G.W. Sheldon, and D.C. Griffiths. 1990. *Climate Change-The IPCC Impacts Assessment*. WMO/UNEP Intergovernmental Panel on Climate Change. Australian Government Publishing Service, Canberra.

USGS EROS Data Center. 1999. USGS 10 Meter Resolution, One-Sixtieth Degree National Elevation Dataset for CONUS, Alaska, Hawaii, Puerto Rico, and the U.S. Virgin Islands. Edition 1. Raster digital data. U.S. Geological Survey Earth Resources Observation and Science, Sioux Falls, SD. Available: <http://gisdata.usgs.net/ned/>. Accessed 7/26/2005.

USGS EROS Data Center. 2001. Landsat ETM+ level-1G SLC-Off Gap-Filled Remote Sensing Image. U.S. Geological Survey Earth Resources Observation and Science, Sioux Falls, SD.

Watson, R.T., M.C. Zinyowera, and R.H. Moss (eds.). 1996. *Climate Change 1995: The IPCC Second Assessment Report, Volume 2: Scientific-Technical Analyses of Impacts, Adaptations, and Mitigation of Climate Change*. Cambridge University Press, Cambridge, UK.

Wigley, T.M.L. 2004. MAGICC/SCENGEN. National Center for Atmospheric Research, Boulder, CO. Available: <http://www.cgd.ucar.edu/cas/wigley/magicc/>. Accessed 10/5/2006.

Wigley, T.M.L. 2006. Assessing the skills of climate models (AOGCMS). Appendix D in *Climate Change and Aspen: An Assessment of Impacts and Potential Responses*. ISBN 0-

9741467-3-0. Prepared for the City of Aspen by the Aspen Global Change Institute, Center of the American West, Rural Planning Institute, Stratus Consulting Inc., and Wildlife & Wetland Solutions, LLC. Aspen Global Change Institute, Aspen. July.

WRCC. 2006a. Alta, Utah (420072). Period of Record Monthly Climate Summary. Available: <http://www.wrcc.dri.edu/cgi-bin/cliMAIN.pl?ut0072>. Accessed 12/28/2006.

WRCC. 2006b. Logan Utah State Univ., Utah (425186). Period of Record Monthly Climate Summary. Available: <http://www.wrcc.dri.edu/cgi-bin/cliMAIN.pl?ut5186>. Accessed 12/28/2006.

WRCC. 2006c. Mountain Dell Dam, Utah (425892). Period of Record Monthly Climate Summary. Available: <http://www.wrcc.dri.edu/cgi-bin/cliMAIN.pl?ut5892>. Accessed 12/28/26006.

WRCC. 2006d. Salt Lake City NWSFO, Utah (427598). Period of Record Monthly Climate Summary. Available: <http://www.wrcc.dri.edu/cgi-bin/cliMAIN.pl?ut7598>. Accessed 12/28/2006.

WRCC. 2006e. Silver Lake Brighton, Utah (427846). Period of Record Monthly Climate Summary. Available: <http://www.wrcc.dri.edu/cgi-bin/cliMAIN.pl?ut7846>. Accessed 12/28/2006.

---

## A. Brief Description of SRES Storylines and Associated Scenarios

The IPCC developed a Special Report on Emission Scenarios (SRES) to provide more consistent projections of greenhouse gas (GHG) emissions – projections that considered the complex social, economic, and technological relationships that underlie energy use and resulting emissions. The SRES approach aimed for an underlying consistency of these complex relationships. The result was a set of logical storylines that encompass the social and physical relationships driving GHG emissions (Nakicenovic and Swart, 2000). For more details on these storylines and scenarios, please refer to the IPCC report at <http://www.grida.no/climate/ipcc/emission/>.

At the core of the SRES approach are four poles along two major axes:

- ▶ Economic vs. environment
- ▶ Global vs. regional.

As shown in Figure A.1, combinations of these four poles give rise to four primary storylines:

- ▶ A1 – Economic growth and liberal globalization
- ▶ A2 – Economic growth with greater regional focus
- ▶ B1 – Environmentally sensitive with strong global relationships
- ▶ B2 – Environmentally sensitive with highly regional focus.

Each storyline describes a global paradigm based on prevalent social characteristics, values, and attitudes that determine, for example, the extent of globalization, economic development patterns, and environmental resource quality. The storylines are by their nature highly speculative. Nonetheless, they do provide identifiable starting points that are defined and consistent with available datasets for some projecting some variables (most notably population, income, land use, and emissions). They have been used in previous and ongoing assessments and provide a basis for intercountry comparisons.

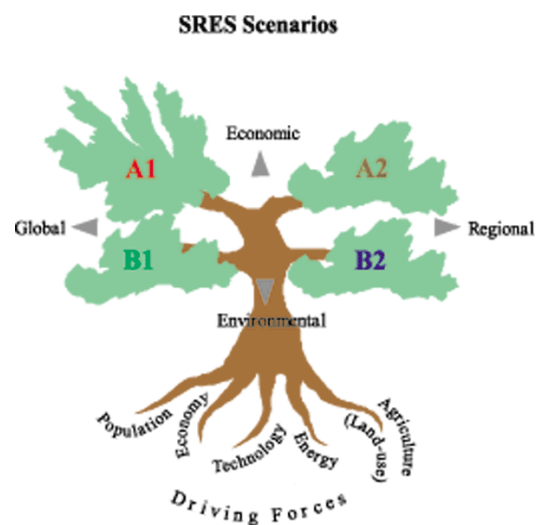


**Figure A.1. Conceptual relationships underlying the SRES scenarios.**

Source: Nakicenovic and Swart, 2000.

The A1 and B1 storylines focus on global solutions to economic, social, and environmental sustainability, with A1 focusing on economic growth and B1 focusing on environmental sensitivity. A2 and B2 focus on regional solutions with strong emphasis on self-reliance. They differ in that A2 focuses on strong economic growth and B2 focuses on environmental sensitivity. The IPCC describes their differences as follows: “While the A1 and B1 storylines, to different degrees, emphasize successful economic global convergence and social and cultural interactions, A2 and B2 focus on a blossoming of diverse regional development pathways.”

The A1 storyline, in general, assumes strong economic growth and liberal globalization characterized by low population growth, very high GDP growth, high-to-very high energy use, low-to-medium changes in land use, medium-to-high resource availability (of conventional and unconventional oil and gas), and rapid technological advancement. The A1 scenario assumes convergence among regions, including a substantial reduction in regional differences in per capita income in which the current distinctions between “poor” and “rich” countries eventually dissolves; increased capacity building; and increased social and cultural interactions. A1 emphasizes market-based solutions, high savings, and investment, especially in education and technology, and international mobility of people, ideas, and technology.

The A1 storyline is broken up into scenarios that characterize alternative developments of energy technologies. A1FI represents the “fossil intensive” scenario and results in the highest emissions and the highest atmospheric concentrations of carbon dioxide (Schröter, 2005). The A1B scenario represents a “balanced” development of energy technologies. It assumes that no one energy source is relied on too heavily and that similar improvement rates apply to all energy supply and end use technologies (Nakićenović and Swart, 2000).

The A2 storyline describes a world with regional economic growth characterized by high population growth, medium GDP growth, high energy use, medium-to-high changes in land use, low resource availability of conventional and unconventional oil and gas, and slow technological advancement. This storyline assumes a very heterogeneous world that focuses on self-reliance and the preservation of local identities, and assumes that per capita economic growth and technological change are more fragmented and slower than in other scenarios. The A2 storyline only has one scenario, so the terms A2 storyline and A2 scenario are used synonymously.

The B1 storyline describes a convergent world that emphasizes global solutions to economic, social, and environmental sustainability. Focusing on environmental sensitivity and strong global relationships, B1 is characterized by low population growth, high GDP growth, low energy use, high changes in land use, low resource availability of conventional and unconventional oil and gas, and medium technological advancement. The B1 storyline assumes rapid adjustments in the economy to the service and information sectors, decreases in material intensity, and the introduction of clean and resource-efficient technologies. A major theme in the B1 storyline is a high level of environmental and social consciousness combined with a global approach to

sustainable development. The B1 storyline only has one scenario, so the terms B1 storyline and B1 scenario are used synonymously.

The B2 storyline, like the A2 storyline, focuses on regional solutions to economic, social, and environmental sustainability. The storyline focuses on environmental protection and social equality and is characterized by medium population and GDP growth, medium energy use, medium changes in land use, medium resource availability, and medium technological advancement. Similar to the A2 and B1 storylines, the B2 storyline has only has one scenario, so the terms B2 storyline and B2 scenario are used synonymously.

---

## **B. Five Selected GCM Simulations of Current Climate and Observed Climate**

Figures B.1 and B.2 display observed temperature and precipitation for the two grid boxes in the central Rockies and the simulations of current climate in the five models. All data are from MAGICC/SCENGEN. Note that the seasonality of precipitation is quite different from precipitation patterns in Park City (which have a wetter, more cyclical pattern). This reflects an average of temperature and precipitation in a grid box going as far north as Montana. All five models closely simulate the seasonality of observed temperatures, although model errors range from 0.03° to 7.03°C in individual months.

For precipitation, the models' performance is more mixed. All five models overstate precipitation in 2000, and three of the five models show a peak in December while observed precipitation decreases in December. The magnitude of the observed precipitation is more closely simulated, with errors ranging from 0.01 mm to 1.58 mm.

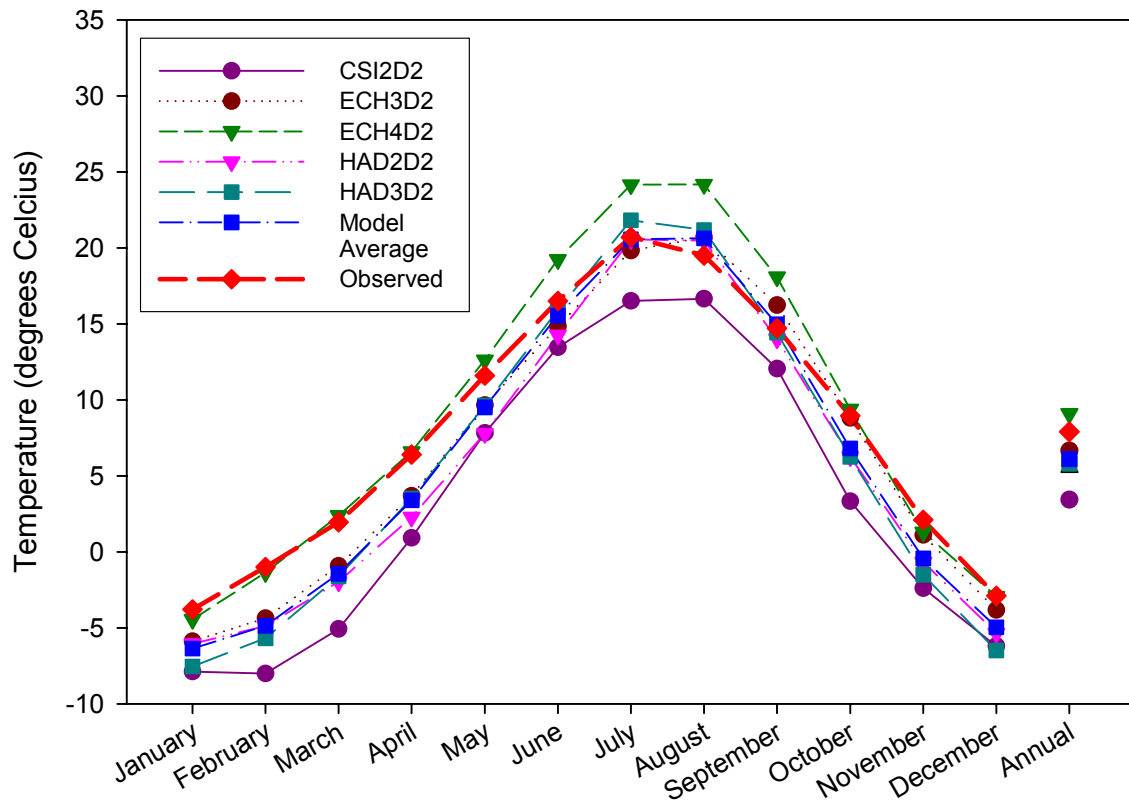


Figure B.1. Modeled vs. observed current (2000) temperature for the Central Rockies.

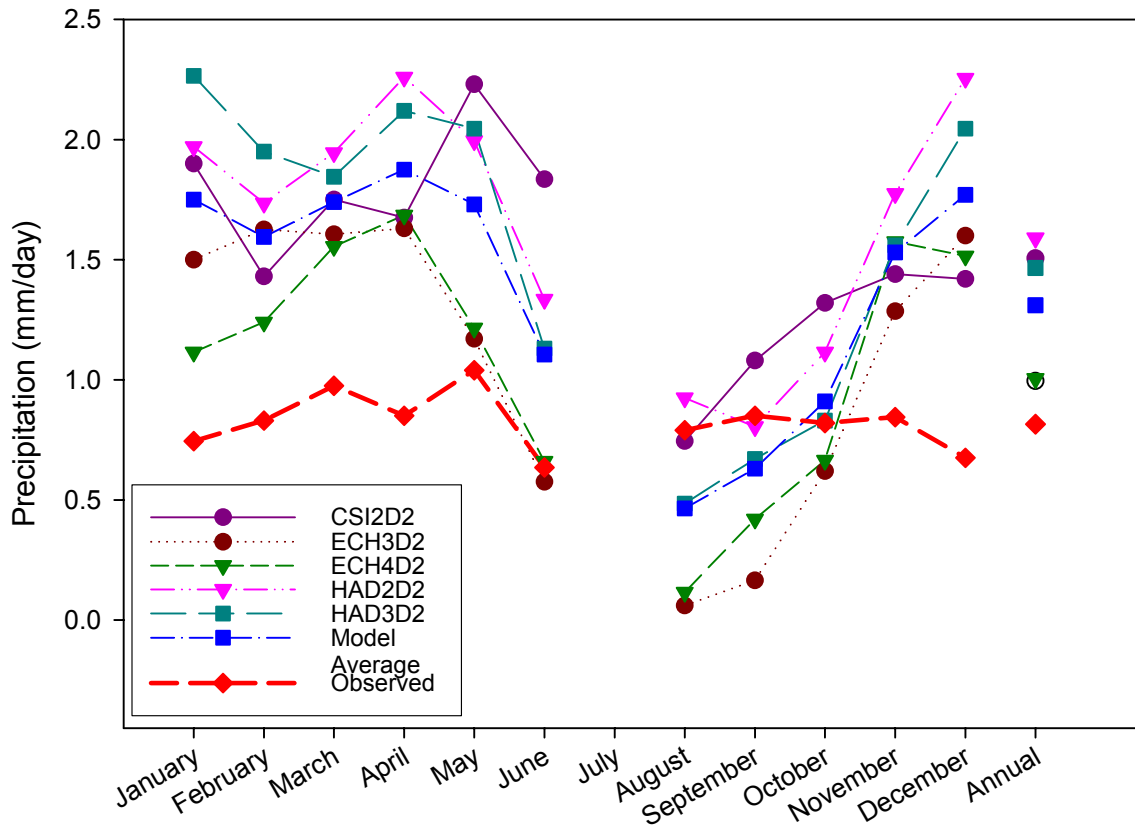


Figure B.2. Modeled vs. observed current (2000) precipitation for the Central Rockies.

---

## C. SDSM Calibration for Thaynes Canyon, 1988-2000

Authored by Dr. Robert Wilby

### C.1 Comment on Data Quality

Observed daily TAVG and PRCP series were taken from the SNOTEL station at Thaynes Canyon, Utah (40.6236°N, 111.53°W, 9230 feet). The data begin in 24 June 1988, and are available to 30 September 2006.

The records were screened for outliers, data entry errors and internal consistency. This led to the removal of suspect high TAVG values ( $> 40^{\circ}\text{C}$ ) between 1 June 1993 and 16 July 1993. One suspect low TAVG ( $-51.4^{\circ}\text{C}$ ) on 29 October 1993 was removed.

SDSM was calibrated against the remaining data for the period 1988-2000. Data are available for the year 2001 onwards, but were not used on the assumption that climate change(s) could be present in the record. Table C.1 shows the NCEP re-analysis predictors selected for model calibration, and the partial correlations of each variable with daily TAVG and PRCP.

**Table C.1. NCEP predictor variables for the grid-box centered on 40°N, 112.5°W**

Predictand	Predictors (NCEP re-analysis)	Partial $r$
TAVG	Mean sea level pressure (MSLP)	-0.82
	Near surface divergence (DSUR)	0.41
	Meridional wind component at 500 hPa level (V500)	0.29
	500 hPa geopotential height (H500)	0.96
PRCP <sup>a</sup>	Relative humidity at 500 hPa level (R500)	0.25
	Vorticity at 500 hPa level (Z500)	0.09
	Zonal wind component at 850 hPa level (U850)	0.26
	500 hPa geopotential height (H500)	-0.16

a. Fourth root transformation for rainfall amount process.

---

## C.2 Biases in Summer TAVG Downscaling Predictor Variables

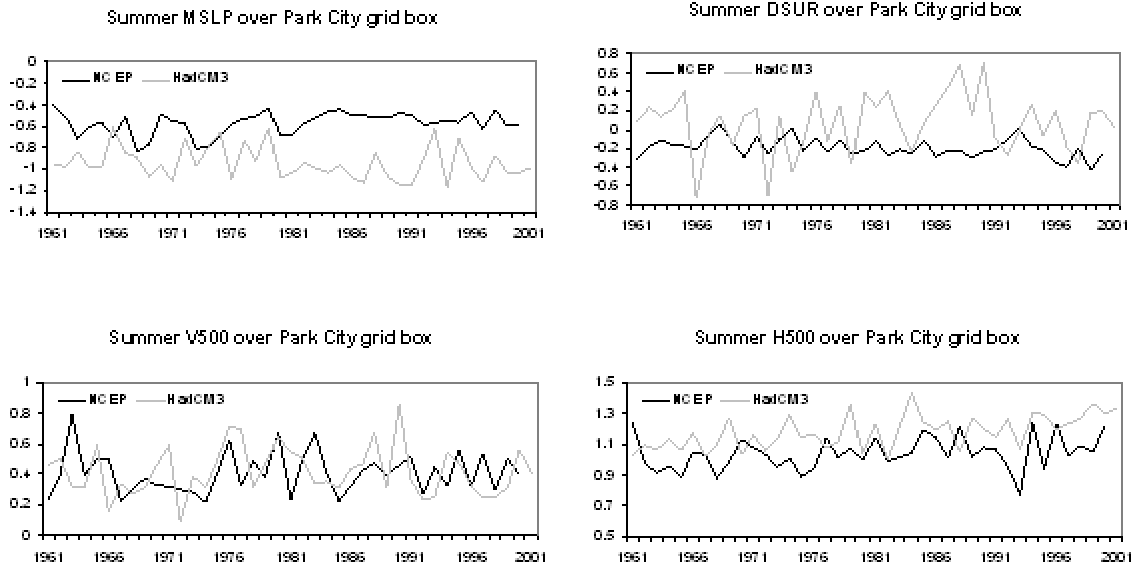


**Figure C.1. Comparison of summer mean NCEP and HadCM3 A2 run predictor variables for the grid-box centered on 40°N, 112.5°W. The most significant biases in HadCM3 summer predictors are in MSLP (negative) and DSUR (positive).**

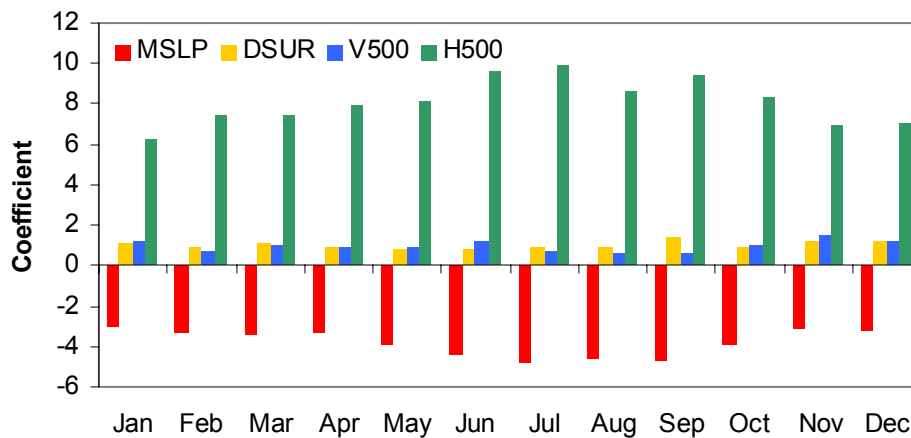


**Figure C.2. Predictor variable weights for TAVG calibrated against NCEP.**

### C.3 Thaynes Canyon Daily Average Temperature (TAVG)

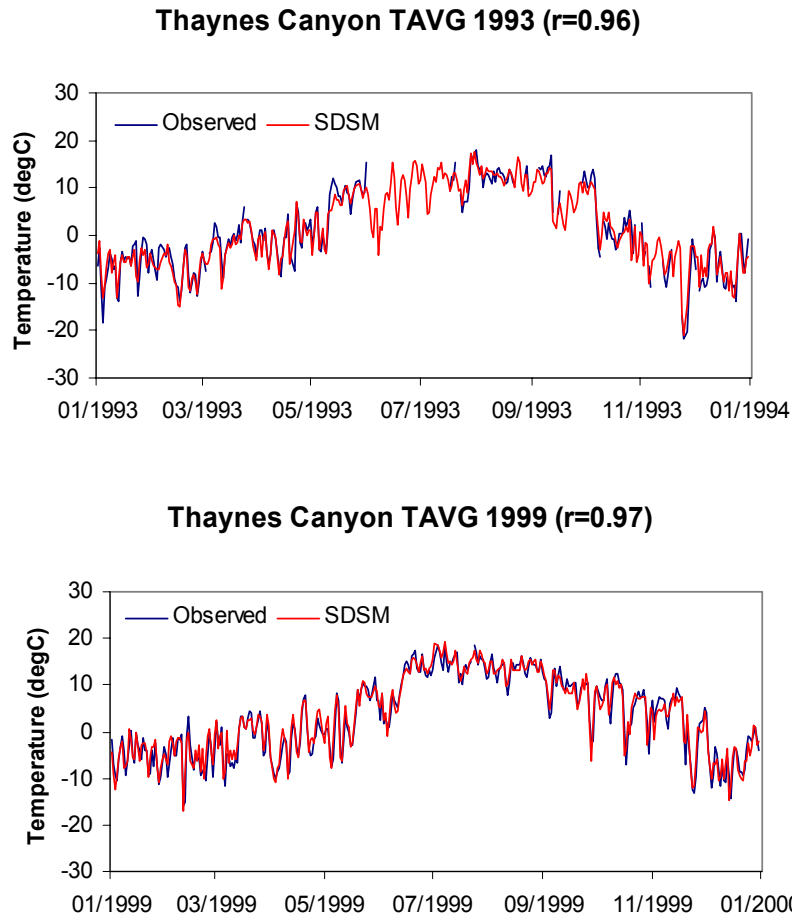


**Figure C.3. Illustration of daily time-series behavior: Comparison of downscaled and observed TAVG for 1993 and 1999. Note the missing data in the summer of 1993.**

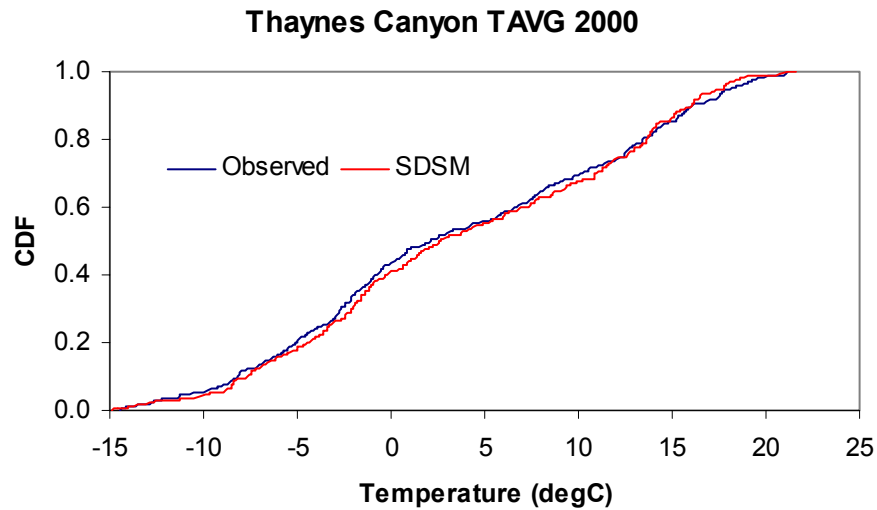


**Figure C.4. Illustration of cumulative distribution function (CDF): Comparison of downscaled and observed daily TAVG for 2000 (the warmest year in the training set).**

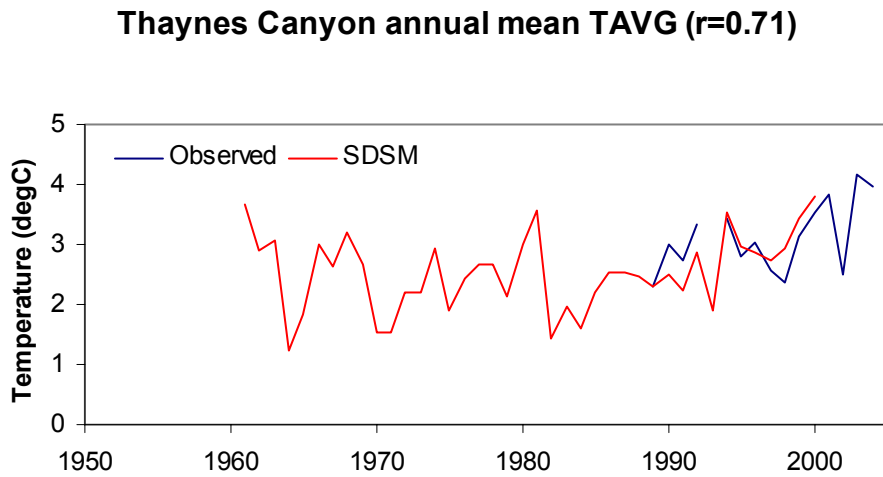


**Figure C.5. Observed and downscaled annual mean TAVG.** Note that the hindcast downscaling was performed using large-scale NCEP predictor variables 1961-2000.

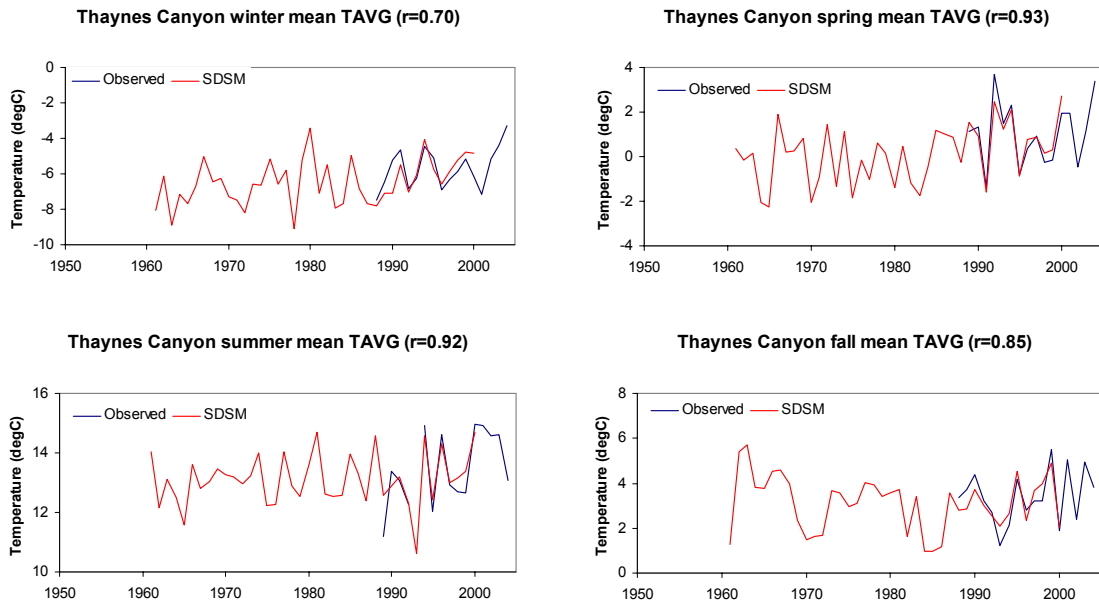


**Figure C.6. Observed and downscaled seasonal mean TAVG.** Note that the downscaling was performed using large-scale NCEP predictor variables 1961-2000.

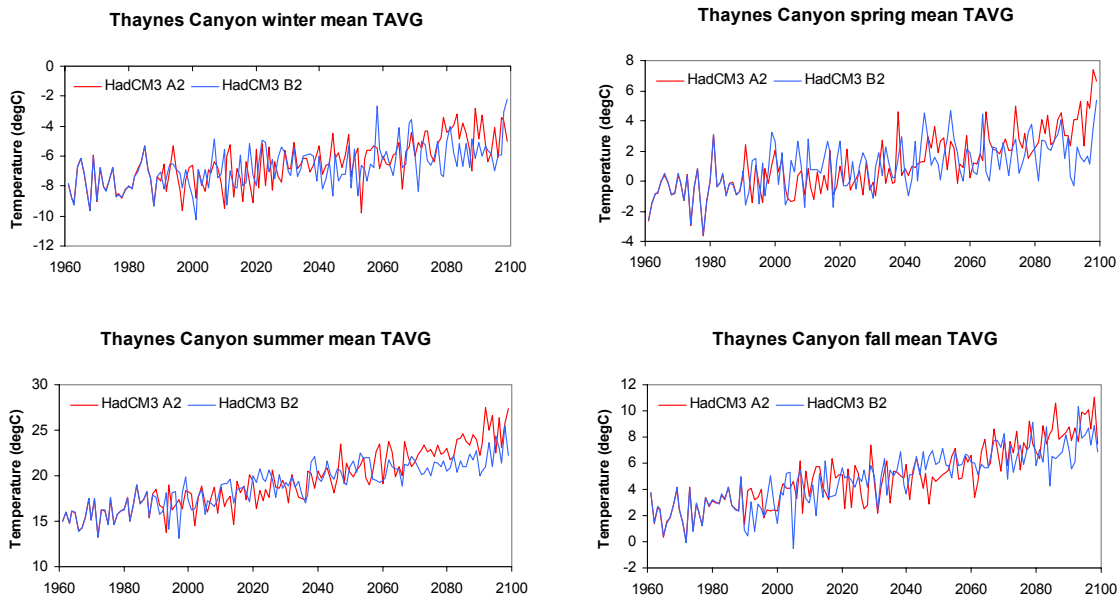


**Figure C.7. Seasonal mean TAVG 1961-2099 downscaled from HadCM3 output under SRES A2 and B2 emissions.**

**Table C.2. Changes in seasonal mean TAVG (°C) for HadCM3, A2, and B2 emissions**

	DJF		MAM		JJA		SON	
	A2	B2	A2	B2	A2	B2	A2	B2
<b>2020s</b>	1.5	1.0	0.9	1.3	2.3	3.0	2.0	2.1
<b>2050s</b>	2.9	1.3	2.3	2.2	4.8	4.5	3.1	3.7
<b>2080s</b>	5.0	2.0	4.0	2.6	7.6	5.4	5.6	4.5
<b>Bias<sup>a</sup></b>	-0.9	-0.9	-0.4	-0.4	3.1	3.0	-0.6	-0.6

a. Estimated with respect to TAVG downscaled from NCEP re-analysis 1961-1990.

## C.4 Thaynes Canyon Daily Precipitation (PRCP)

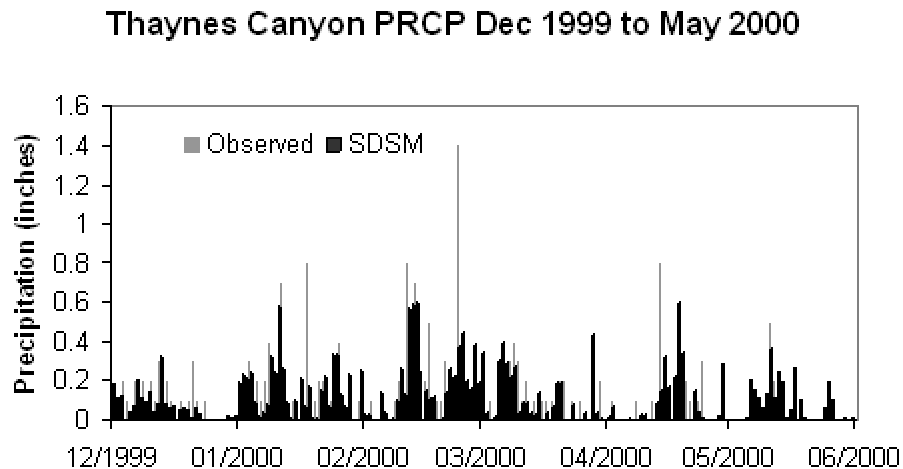


**Figure C.8. Illustration of daily time-series behavior: Comparison of downscaled and observed PRCP for the winter/spring of 1999/2000.**

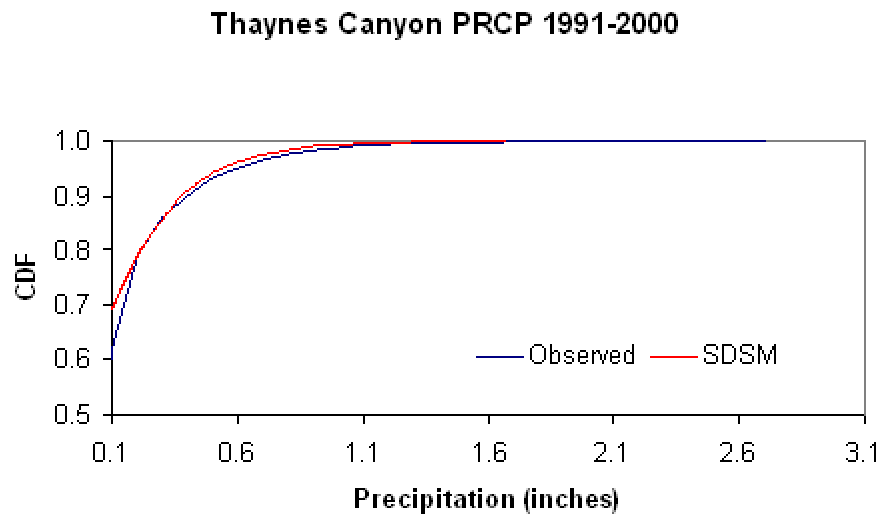


**Figure C.9. Illustration of cumulative distribution function (CDF): Comparison of downscaled and observed daily PRCP for 1991-2000.** Note that SDSM gives the fraction of days with nonzero precipitation (~37%) compared with observed (~38%).

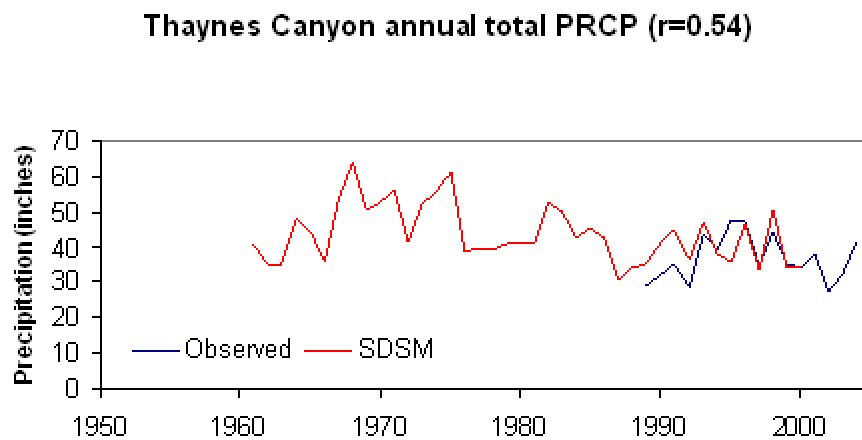


**Figure C.10. Observed and downscaled annual PRCP.** Note that the downscaling was performed using large-scale NCEP predictor variables 1961-2000.

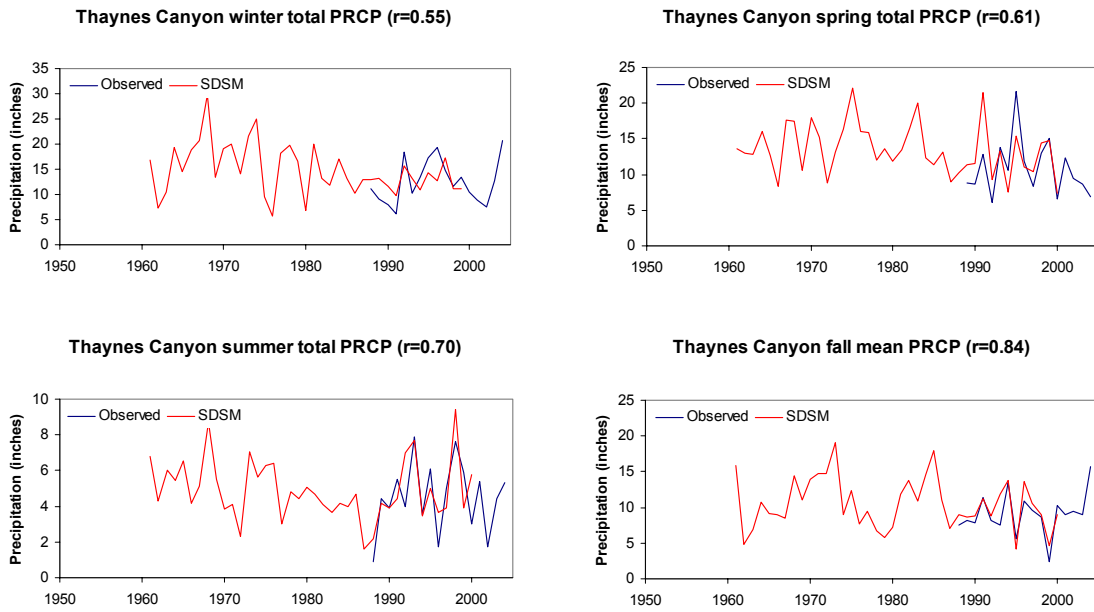


**Figure C.11. Observed and downscaled seasonal total PRCP.** Note that the downscaling was performed using large-scale NCEP predictor variables 1961-2000.

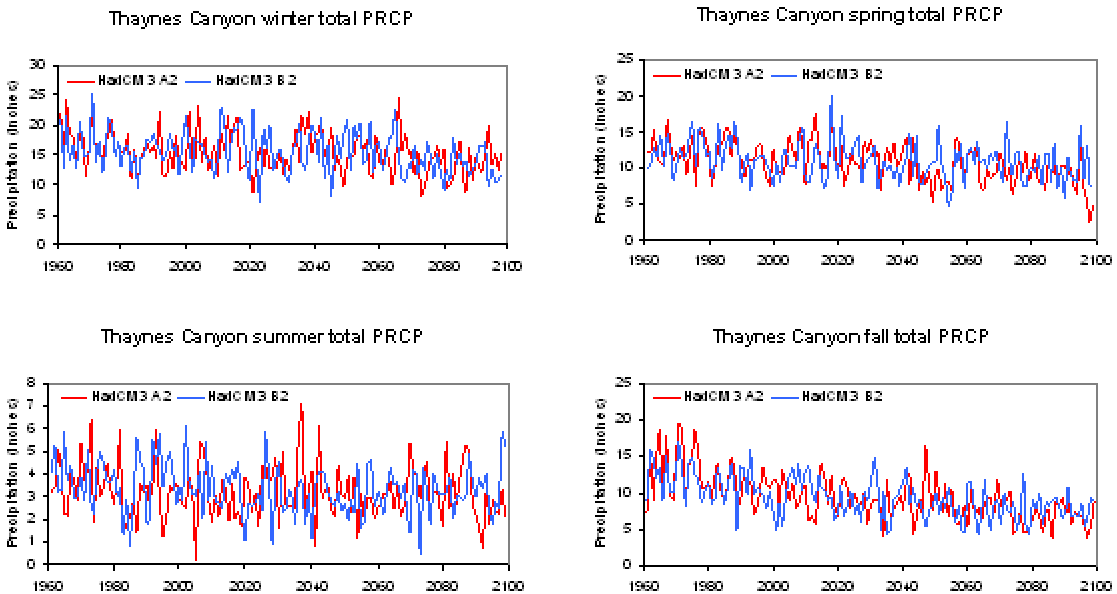


**Figure C.12. Seasonal total PRCP 1961-2099 downscaled from HadCM3 output under SRES A2 and B2 emissions.**

**Table C.3. Changes in seasonal total PRCP (%) for HadCM3, A2, and B2 emissions**

	DJF		MAM		JJA		SON	
	A2	B2	A2	B2	A2	B2	A2	B2
<b>2020s</b>	-4	0	-6	-12	-7	-16	-30	-19
<b>2050s</b>	-7	-3	-21	-13	-13	-14	-31	-30
<b>2080s</b>	-20	-18	-29	-19	-9	-9	-47	-32
<b><i>Bias<sup>a</sup></i></b>	7	5	-10	-11	-28	-24	17	7

a. Estimated with respect to PRCP downscaled from NCEP re-analysis 1961-1990.

## C.5 Summary

### C.5.1 Temperature scenarios

- ▶ Overall, SDSM reproduces > 80% of the daily variation in TAVG at Thaynes Canyon for the period 1988-2000 given only information from atmospheric predictor variables overlying the target region.
- ▶ Relatively poor skill for individual seasons (e.g., summer 1989) is linked, in part, to missing observed data.
- ▶ Hindcast TAVG series downscaled by SDSM from NCEP predictors suggest rapid warming in winter and spring between 1961-2000. Over this period the seasonal temperature change was: +0.4°C/decade (winter and spring), +0.1°C/decade (summer), and -0.2°C/decade (autumn).
- ▶ Warming is expected in all seasons for the 2020s, 2050s, and 2080s under both emission scenarios. The warming is most rapid in summer, but projected rates of warming in winter and spring are comparable to historic rates (see above).
- ▶ The projected temperature changes are relatively high compared with other high elevation stations in the western U.S. (e.g., Niwot Ridge, Independence Pass), but the pattern of most rapid warming in summer is consistent between sites.

- ▶ The high rates of warming at Thaynes Canyon could be an artifact of the large bias (+3°C) in the scenarios downscaled from HadCM3 predictors when compared with NCEP predictors for 1961-1990. The difference in downscaled TAVG was attributed to a significant negative bias in HadCM3 MSLP, and positive bias in DSUR compared with NCEP.
- ▶ The bias due to downscaling predictors is less than 1°C in other seasons.

### C.5.2 Precipitation scenarios

- ▶ Predictability of daily and seasonal PRCP totals at Thaynes Canyon using regional NCEP variables is less than TAVG.
- ▶ Assessment of model skill for inter annual and inter decadal totals was not possible due to the short observation record.
- ▶ Despite the brevity of the calibration set, SDSM produces realistic daily time-series of precipitation occurrence and wet-day totals. Overall, the model tends to underestimate the frequency of heavy precipitation events (> 1 inch/day).
- ▶ Biases in PRCP totals due to downscaling predictor variables (i.e., NCEP compared with HadCM3) were greatest in summer, and least in winter/ spring.
- ▶ With the above in mind, future projections based on HadCM3 output suggest less precipitation in all seasons. However, the largest reductions are expected in fall and spring and to a less extent in winter and summer.

---

## D. GIS/Remote Sensing Methods

### Methods used to generate digital elevation model and elevation classes

Here we describe the methods used to generate the elevation zones and snow-covered area estimates required for the snowpack modeling. The characterized elevation zones and snow coverage values are input parameters used in the Snowpack Runoff Model (SRM). For the elevation input parameter, ten foot contour digital data (McReynolds, 2006) for the ski area were converted to a 10 m cellsize digital elevation model (DEM) after generating a Triangulated Irregular Network (TIN) dataset. The DEM was then subset to the boundary of the ski area and classified into the following four elevation zones:

- ▶ 6,889-7,680 ft
- ▶ 7,680-8,560 ft
- ▶ 8,560-9,440 ft
- ▶ 9,440-10,400 ft.

Total area and minimum, maximum, and mean elevation statistics were then generated for each elevation zone for use in the SRM model.

In addition to the ski area DEM, 10 m resolution DEM data from the U.S. Geological Survey's (USGS's) National Elevation Dataset (NED) were downloaded from <http://gisdata.usgs.net/ned/> for the area that includes Park City (USGS EROS Data Center, 1999). The two DEMs were combined into a single dataset that was used in the orthorectification of imagery used to generate snow cover estimates mentioned below.

### Methods used to generate snow cover data

Snow cover was estimated using satellite data. One Landsat 7 Enhanced Thematic Mapper (ETM+) level 1G SLC-off gap filled scene, and five Landsat 5 Thematic Mapper (TM) scenes were acquired from USGS EROS Data Center (2001). The scenes covered the following dates: October 19 (ETM+) and December 30, 2000 for the early season, and January 31, March 4, April 5, and May 7, 2001 for the late season.

Six Landsat bands (1-5, 7), covering the visible to short wave infrared (SWIR) portion of the electromagnetic spectrum, were imported into ERDAS Imagine software (v.8.7) and combined into six respective multispectral images. Each image was then orthorectified as follows. Ten locations on the imagery were co-located with locations on an existing orthorectified summer (August 14, 1999) Landsat 7 ETM+ image (band 8, 14.25 m cellsize) (GLCF, 2004) and used as ground control points to georeference the unreferenced imagery to real-world locations. To

correct for terrain displacement, the DEM was used as input into the orthorectification process. In processing the data, the nearest-neighbor method was used during resampling.

The orthorectified imagery was then used as input to derive the snow-covered area. The Normalized Difference Snow Index (NDSI), which exploits the high reflectance in wavelengths where snow is bright (green, 0.525-0.605  $\mu\text{m}$  Landsat) vs. wavelengths where snow is dark (SWIR, 1.55-1.75  $\mu\text{m}$  Landsat), was used to identify snow cover and was calculated as follows:

$$NDSI = (TM \text{ band}2 - TM \text{ band} 5) / (TM \text{ band}2 + TM \text{ band}5) \quad (1)$$

As the NDSI ratio tends to falsely classify dark areas in the imagery as snow, shadows and densely forested areas were classified as non-snow areas. The near-infrared band (TM band 4, 0.75-0.90  $\mu\text{m}$ ) was used to differentiate the lighter areas from those areas either in shadow or partially to fully forested (Klein et al., 1998; Dozier and Painter, 2004). Values used to subset the imagery were specific to each image and determined through visual comparison between the area identified and visual interpretation of the raw imagery, but ranged from ~8% to 23% of digital number (DN). After masking out the dark areas from the imagery, snow-covered areas were identified using an NDSI value greater than 0.3.

Lastly, the snow-covered area was overlaid with the four-classed elevation layer to calculate the percent snow cover by elevation class.